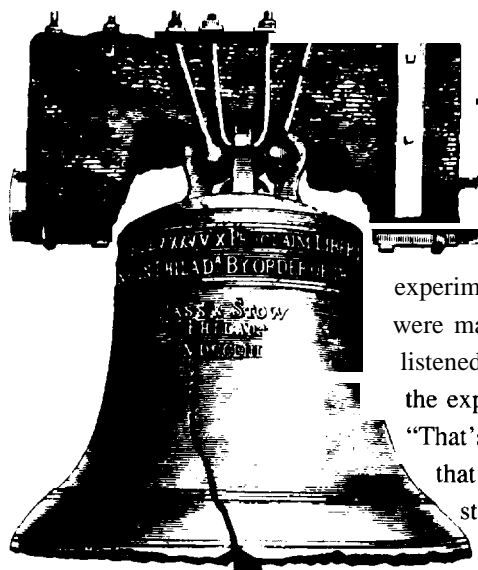# NEUTRONS, SLUDGE PHYSICS
and the
LIBERTY BELL *by Roger Pynn*

A friend of mine, a well-respected theoretical physicist at a major American university, worked for many years on polymers and colloids at one of the better-known oil companies. He told me that he once discussed his work with an equally well-respected experimentalist whose main preoccupations were magnetism and phase transitions. Having listened to my theorist friend for a few minutes, the experimentalist rendered his verdict: "That's sludge science!" He meant, of course, that the polymers and colloids my friend studied did not have a convenient monocrystalline form-their physical properties were not simplified by a symmetrical atomic arrangement. Traditionally, scientists have preferred

Why would one want to study sludge with neutrons? Our opener shows both high-tech and mundane products made of disordered materials washing in on a blue wave of sludge. In the background, fumed silica particles (red) represent the fractal aggregates elucidated by neutron scattering. The Liberty Bell, a famous example of the effects of residual stress, rounds out this gallery of neutron scattering's practical applications.

to investigate the physical properties of ordered systems, or at least of materials that are free of impurities and dirt. Unfortunately, many of the materials on which our society depends are "dirty" and quite devoid of the translational symmetry of a crystal—they are made of "sludge."

Examples of sludge abound: the oil we put in our automobile engines with all of the detergent additives that advertisements insist are so important; the various polymers we use to package food, weave cloth, make compact disks, and produce a variety of parts for dishwashers, televisions, and other appliances; the paints and cosmetics we use to color and preserve our houses and our skins; detergent; soap; toothpaste; even some things that pass for food. In today's age of advancing technology, we are constantly seeking new materials that can better serve our needs, that can carry out a new or an old function better than existing materials.

But why would one want to study sludge with neutrons? To design new materials we have to understand the relationships between material properties, material structure, material synthesis, and material performance (Fig. 1). As an example, we may decide that the steel armor of yore is impractical for the modern policeman. Instead, we need a flack-jacket that is strong enough to stop bullets, flexible enough to let the policeman move his arms, and light enough for him to go to battle without a horse. Our dream material needs to combine all these properties. Polymers—a common type of sludge—are light and flexible, but those we encounter daily as zip-lock bags or the outer casings of televisions are not strong enough. To design a polymer with the strength to stop bullets requires an understanding of the relationship between molecular structure and strength. Once we know the structure that provides the strength we want, we have to invent a way of

synthesizing a polymer with that structure. Neutrons enter the picture because they often provide an ideal method of determining the structures of materials. We may not think of sludge as having structure, and none may be visible to the naked eye, but the molecules are always organized in some way, and that organization often determines properties.

Structure, properties, synthesis: all investigations build to the performance apex of the materials research pyramid. Once we make a product from our dream material, we must find a way to ensure that it will perform adequately. For a unique, expensive product we must make this guarantee without simulating future use—which brings us to the Liberty Bell. Some years after its manufacture, the Liberty Bell cracked, probably as a result of stresses introduced when it was cast. Without realizing that their bell's fame would hang from its failure, the manufacturers might have prevented the rupture if they had understood the distribution of stresses related to the casting process. However, to achieve such an understanding without destroying the Bell or any other stressed piece of metal—a railway line, an oil pipeline, or a turbine blade—is difficult. We have to measure the strain in the material, that is, the amount by which it has been stretched or compressed during manufacture. or use, without disturbing an atom. Unfortunately, most of the traditional methods employed to obtain information about residual strains involve destruction or modification of the component—hole drilling in conjunction with strain-gauge measurements and progressive removal of layers of material, for example. Today, neutron diffraction provides an alternative, nondestructive method of measuring changes in the interatomic spacings, and thus of measuring the residual strains, at different positions in the sample.

In this article I will describe a few

of neutron scattering's contributions to our understanding of the structures of several different types of sludge and to studies of the stresses in metals. Experiments of this sort are relatively new to neutron scattering. The profound contributions that neutrons have made to polymer science—such as determining the conformations of polymer molecules—started at the beginning of the seventies, and neutron measurements of residual strains in engineered components began only in the eighties. To a small extent this evolution has depended on the development of instrumentation for neutron scattering. To a far larger extent it results from a maturing of the field. In the early days, neutron-scattering researchers measured single crystals and tried to understand the properties described in graduate texts on physics: atomic and magnetic structures of inorganic solids, phonons and magnons in crystals, and the structures of simple liquids, for example. Later, they used neutrons to study the structural aspects of much more esoteric phenomena—structural phase transitions, manifestations of nonlinearity such as solitons, and the coexistence of magnetism and superconductivity. Each new phenomenon left its signature on neutron-scattering experiments by giving rise to a qualitatively different neutron scattering law. Each was a stepping stone to the study of a more complex system. Now the technique is mature enough to apply to sludge, to materials we really care about.

Of course, as a practicing scientist I strongly believe basic research should be pursued, even when its relevance to society is not instantly apparent. From lignite to lasers, most of the discoveries that have profoundly affected our lives have resulted from simple human inquisitiveness, not from a desire to make a better widget. It is important that neutron scattering continue to be used for basic research—witness the other ar-

(a) Essential Areas of Study
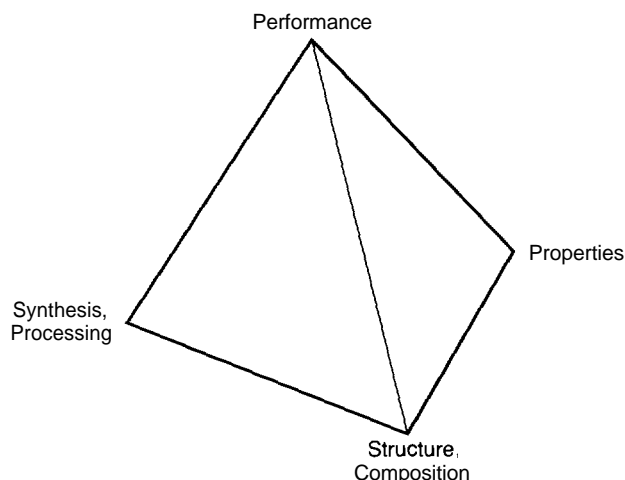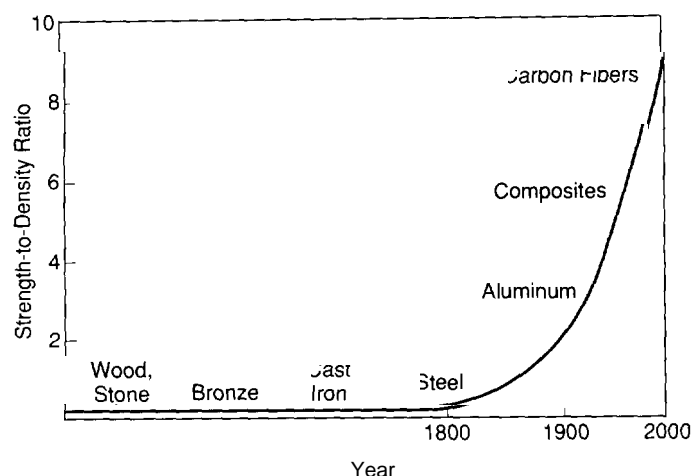
MATERIALS RESEARCH

Fig. 1. (a) This tetrahedron represents the four essential areas of materials research. Its symmetry implies that investigations of any apex must necessarily build on the other three. For example, the sharp improvement in the strength-to-density ratio of construction materials—shown on a relative scale in (b)—would not have been possible without concurrent advances in methods for synthesizing new materials, elucidating their structures, clarifying their properties, and testing their performance. Of course, the complicated demands of high-technology applications require attention to more than just strength and weight. As a simple example, lightweight composite materials that get stronger when heated are being developed for the wings and engine of hypersonic jets. (The graph is reprinted from *Materials Science and Engineering in the 1990s*, @1989 by the National Academy of Sciences, National Academy Press, Washington, D. C.)

ticles in this issue. However, when a technique can make significant contributions to the solution of more immediate and practical problems, those problems should not be ignored. They are certainly no less challenging intellectually, and their solutions have immediate, obvious impact. Such studies contribute to incremental improvements in our technologies, while basic research often drives the revolutionary changes that become clear in hindsight.

Colloids and Amphiphilic Molecules

The first type of sludge I will discuss is colloidal sludge. A colloid is an assembly of small particles dispersed in a continuous medium of gas, liquid, or solid. Fog, smoke, milk, paint, and foam are colloidal systems encoun-

tered routinely. Because the particles are small—between 10 and 10,000 angstroms (1 angstrom = 10^-10 meter)—they do not settle even when dispersed in gases or liquids. Rather they are kept in suspension by the kicks they receive from molecules of the carrier fluid. Many macromolecules such as polymers or proteins dissolve easily in a solvent, and in this case the colloidal particles are the molecules themselves. More fascinating and technically relevant are the so-called association colloids, one class of which consists of aggregates of relatively small *amphiphilic* molecules. Amphiphilic molecules have a polar, and hence water-soluble. head at one end and a water-insoluble tail at the other; the head is *hydrophilic*-water-loving—whereas the tail is *hydrophobic* -water-hating. In water such molecules aggregate so that their tails
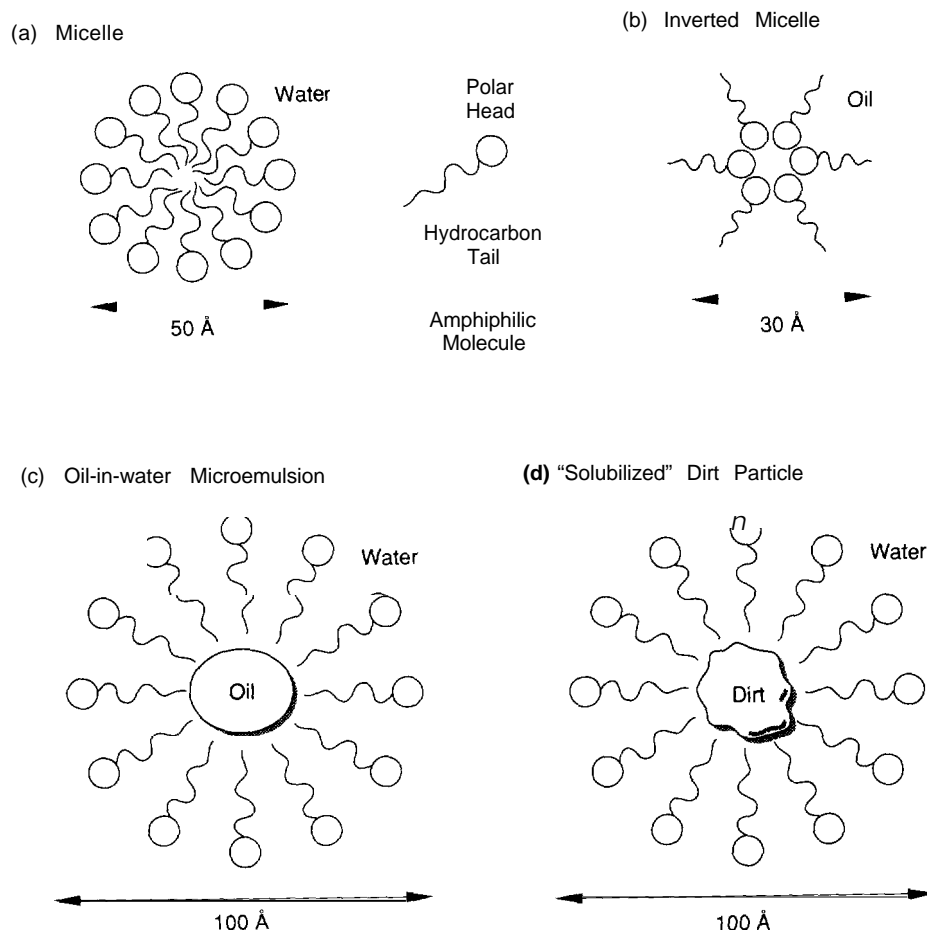
are dry, assembling spontaneously into particles called *micelles* (Fig. 2). In addition, amphiphilic molecules solubilize materials that are normally completely insoluble in water—metals, ceramics, or oils, for example. The amphiphilic molecules are adsorbed onto the sur-faces of "dirt" particles, and these surface layers prevent the dirt from separating out. Like the micelle, this configuration prevents contact between the. tails of the amphiphilic molecules and the water environment. When small groups of amphiphilic molecules solubilize a liquid, such as oil, the resulting colloid is called a *microemulsion.*

Anyone who has tried to wash clothes or dishes in plain water knows why amphiphilic molecules are important: without soap or detergent—amphiphilic molecules by another name-dust and grease will not wash away. In addition

(a) Micelle

Water

Polar
Head

(b) Inverted Micelle

Oil

Hydrocarbon
Tail

50 Å

Amphiphilic
Molecule

30 Å

(c) Oil-in-water Microemulsion

Water

Oil

100 Å

(d) "Solubilized" Dirt Particle
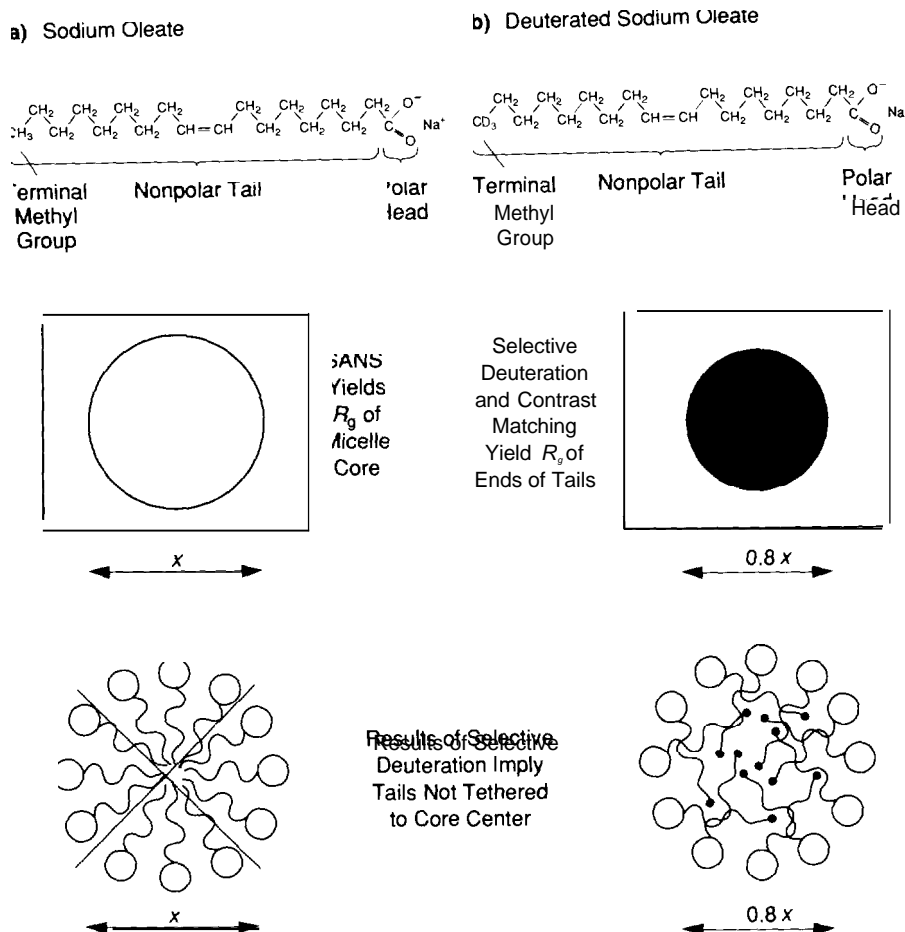
Water

Dirt

100 Å

TYPES OF ASSOCIATION COLLOIDS

Fig. 2. When a sufficient number of amphiphilic molecules are dispersed in a solvent, the interaction between their hydrophilic heads and hydrophobic tails and the solvent molecules can lead to formation of various types of colloidal particles. (a) In water amphiphilic molecules can form micelles in which the hydrophobic tails group together so that only the polar heads contact the water. (b) In oil the opposite happens; the polar heads group together so that only the tails contact the oil. (c) Amphiphilic molecules can form a microemulsion of oil in water by surrounding oil droplets with their tails. (d) Detergent molecules can make dirt particles soluble in water by surrounding them. Although the effects of the hydrophobic and hydrophilic interactions suggest the general configuration of the colloidal particles, techniques such as x-ray and neutron small-angle scattering are needed to study details of size, shape, and structure.

to everyday dirt, amphiphilic molecules are used to solubilize a wide variety of other materials. Detergents isolate corrosive products in motor oil by forming microemulsions; light-sensitive emulsions register images in photographic processes; bilayers of amphiphilic molecules are used to encapsulate drugs for more efficient delivery in the body; microemulsions are used for tertiary oil recovery by the petroleum industry: and fats are transported in our blood stream by micelles formed from serum lipoproteins—the high-density lipids we hear about in connection with our cholesterol measurements.

In describing the association colloids that can be made with amphiphilic molecules, I have given in Fig. 2 the conventional textbook cartoons that purport to describe the structures of various colloidal particles. However, the cartoons gloss over many important questions. For instance, are the particles really spherical? How big are they? Are all particles in a colloidal suspension the same size? How much of the particle volume is occupied by the head groups? How much by the tails? Is the tail region uniformly dense? What is the effective surface charge? How do the particles organize themselves in concentrated suspensions? And how do all of these properties depend on temperature and the concentration of amphiphilic molecules? Many of these questions can be answered by small-angle neutron-scattering (SANS) experiments, especially when the technique of contrast matching is used.

Small-angle neutron-scattering experiments are useful for measuring lengths between 10 and 10,000 angstroms, the size range in which many colloidal particles fall. As the name implies, researchers measure the intensity of neutrons scattered at very small angles, that is at very small values of the wavevector transfer, Q. For values of Q that are less than about R^{-1} (that is, for

values of QR less than about 1), where R is the approximate size of a particle, the appropriate approximation for the scattering from a dilute suspension of particles is the Guinier approximation, which in logarithmic form is

$$\ln I(Q) = -\frac{1}{3}R_g^2 Q^2 + \ln I(0). \quad (1)$$

$I(Q)$ is the scattering law, that is the intensity of scattered neutrons as a function of Q, and R_g is the so-called radius of gyration of the particle. R_g is analogous to the radius of gyration of classical mechanics (the square of which

equals a body's moment of inertia divided by its mass) and thus is a good measure of particle size. According to the Guinier approximation, we can determine R_g by plotting the logarithm of the scattered-neutron intensity versus $\frac{1}{3}Q^2$. At small values of Q, the plot should be a straight line with a slope of $-R_g^2$. In the case of a solid spherical particle whose size is determined only by one dimension—its radius—that dimension can be obtained directly from R_g; $r = \frac{1}{3}\sqrt{15}R_g$, or about $1.29R_g$. However, more dimensions are needed to define anisotropic shapes such as ellipsoids, cylinders, or pyramids. In these

a) Sodium Oleate

$$CH_3 \, CH_2 \, CH_2 \, CH_2 \, CH_2 \, CH=CH \, CH_2 \, CH_2 \, CH_2 \, CH_2 \, C \overset{O^-}{\underset{O}{\diagdown}} \, Na^+$$

Terminal Methyl Group | Nonpolar Tail | Polar Head

b) Deuterated Sodium Oleate

$$CD_3 \, CH_2 \, CH_2 \, CH_2 \, CH_2 \, CH=CH \, CH_2 \, CH_2 \, CH_2 \, CH_2 \, C \overset{O^-}{\underset{O}{\diagdown}} \, Na^+$$

Terminal Methyl Group | Nonpolar Tail | Polar Head

SANS Yields R_g of Micelle Core

$\longleftrightarrow x \longleftrightarrow$

Selective Deuteration and Contrast Matching Yield R_g of Ends of Tails

$\longleftrightarrow 0.8 x \longleftrightarrow$

Results of Selective Deuteration Imply Tails Not Tethered to Core Center

$\longleftrightarrow x \longleftrightarrow$

$\longleftrightarrow 0.8 x \longleftrightarrow$

DETAILS OF MICELLAR STRUCTURE

Fig. 3. The difference between the neutron scattering lengths of hydrogen and deuterium allows researchers to see the internal structure of micelles in some detail. (a) The hydrocarbon tail of sodium oleate-a common soap—has an almost homogeneous scattering-length density along its entire span. At beat, neutron scattering can show that a micelle consists of an outer shell of head groups and a core of tails with a radius of gyration x. (b) By substituting deuterium for hydrogen in the terminal methyl groups of the sodium oleate and adjusting the scattering-length density of the solvent, researchers can distinguish the ends of the tails from the tails as a whole. The 20-percent smaller radius of gyration obtained for the deuterated methyl groups (red) leads researchers to postulate a less ordered structure for the micellar core. The terminal methyl groups tend toward the center of the micelle but are not heavily concentrated there.

cases, R_g gives a good approximation of the average particle dimension.

In addition to particle size, a Guinier plot can be used to determine $I(0)$, the extrapolated value of the scattering law at $Q = 0$. This value is proportional to the average mass of the colloidal particles, that is, to the average. number of amphiphilic molecules contained in a particle. Thus, simple Guinier analysis of small-angle neutron-scattering data from dilute suspensions provides immediate quantitative information on the average dimension and mass of the colloidal particles.

At larger values of Q, for exam-

ple in the *Porod region* where QR is greater than 5, the intensity of scattered neutrons yields information about the surface structures of colloidal particles. In particular, Porod's law says the scattered-neutron intensity will be proportional to Q^{-4} if the surfaces of the colloidal particles are smooth. Moreover, the constant of proportionality measures the surface area of the colloidal particles per unit volume of suspension. If the scattering law in the Porod region obeys a power law with an exponent between -3 and -4, the colloidal particles have rough surfaces, which need to be described by the frac-

tal concept described later in this article.

In addition to the size and surface area of the colloidal particles, small-angle neutron scattering also allows us to determine some details of their internal structures. For example, Fig. 2 indicates that all the hydrocarbon tails in the micellar core have the same zig-zag conformation and all point toward the center of the micelle. Is this really the case? Probably not, because such an arrangement would allow water to penetrate the micelles and come in contact with the hydrophobic tails. On the other hand, one would not expect the micellar cores to have a uniform, liquid-like density either. After all, the arrangement of the tails is constrained by the distribution of the polar heads on the particle surface. Probably the real situation lies between the two limits. The neutron-scattering technique known as *contrast marching* can help to resolve this issue.

Contrast matching is based on a simple principle: components of particles that have the same density of scattering power, or *scattering-length density,* as the solvent in which the particles are dispersed do not contribute to the observed scattered-neutron intensity. (See "Neutron Scattering—A Primer" and "Biology on the Scale of Neglected Dimensions" for a more detailed account of contrast matching.) If we could somehow match the scattering-length density of the solvent to all regions of the hydrophobic tails except the methyl groups at their ends (see Fig. 3), then the observed scattering would be due to the methyl groups alone and would provide information about their spatial distribution. Achieving that situation is possible because of a fortunate quirk of nature—the relatively large difference between the scattering lengths of hydrogen and deuterium. Researchers substitute deuterium for hydrogen in the terminal methyl groups and disperse the micelles in a mixture of D_2O and H_2O whose scattering-length density closely

matches that of the tails. By this process, researchers can "see" the spatial distribution of the deuterated methyl groups alone. Typically, the radius of gyration found for the deuterated methyl groups in a micelle is less than that of the whole micellar core, indicating that the ends of the molecular tails are more likely to be found toward the center of the micelle than evenly distributed throughout the core. On the other hand the difference between the two values of R_g is typically less than 20 percent. So the ends of the chains are certainly not tethered to the center of the micelle as Fig. 2 indicates.

So far, I have talked only about experiments on generic colloidal systems. To develop colloidal systems for specific applications, we must improve our understanding of the relation between a sample's structure and its properties. As a simple example: it is easy to understand why soap works in terms of Fig. 2-dust or oil are imprisoned by amphiphilic molecules and washed away in a milky dispersion. But suppose, by chance, that even slight dilution of the system caused the soap molecules to release their captives. This structural change would mean that the very action of rinsing off the soap would redeposit all of the dirt! To understand this phenomenon-or develop a better soap-we would need to examine the stability of molecular arrangements as a function of molecular concentration. Neutron scattering can tell us the arrangements amphiphilic molecules assume, but the *free energy* of these arrangements determines their stability.

The free energy of a molecular arrangement is calculated by using the equation

$$F = H - TS . \qquad (2)$$

That is, the free energy, F, equals the sum of the particle-interaction energies, H, minus the temperature, T, times the entropy, S. The arrangement with the lowest free energy is the most stable. Entropy is a measure of disorder and is largest for a random distribution of amphiphilic molecules in solution and smaller for an ordered arrangement such as a micelle. Because T and S are always positive, free energy decreases as entropy and temperature increase. Thus, entropy considerations tend to favor random distributions of' amphiphilic molecules over ordered systems such as micelles, especially at high temperatures. Also opposing micelle formation are the electrostatic forces that come into play when the polar heads of the amphiphilic molecules are constrained to lie on the surface of a micelle; the heads experience repulsive forces which increase the interaction energy (and thus the free energy).

On the other hand, what amounts to an attraction between the hydrophobic tails of the molecules counters the "bumping heads" effect and the effects of entropy and thus favors the formation of micelles. The attraction is thought to be an indirect effect of the interaction between the tails of the amphiphilic molecules and the molecules of the solvent. When amphiphilic molecules are randomly distributed in water, their hydrocarbon tails disrupt many of the water's hydrogen bonds, thereby increasing the solvent's free energy. The water molecules like to restore these bonds and reduce their free energy; so they tend to push the tails out of the way, causing them to group together and form micelles. For many amphiphilic molecules, the effective attraction between the hydrophobic tails is about equal to the repulsion between their polar heads if the concentration of amphiphilic molecules is high enough. The free energy is then lowest when the molecules self-assemble into micelles. However, at high enough temperatures entropy always wins and the molecules are randomly distributed in the solvent.

Vesicles: A Novel Drug Delivery System. Aggregations of amphiphilic molecules can assume more complicated shapes, and the hydrophobic interaction can have a wider variety of effects than simple micelles. For example, commercial applications of the hydrophobic effect include nonwetting, nonstick pans and waterproof fabrics, and the semipermeable membranes of biological cells in our bodies are formed from bilayers of amphiphilic lipid molecules. In addition, one of the most technologically exciting actions of amphiphilic molecules is the formation of hollow, spherical shells called vesicles (see Fig. 4). Vesicles are composed of bilayers of amphiphilic molecules that are very similar in form to the membranes of biological cells and sometimes contain the same lipids. Such vesicles—called *liposomes* -occur naturally in the body and serve a variety of purposes, including the transport of fats during digestion.

The idea of using liposomes for drug delivery was born in the late 1960s as a possible solution to one of medicine's fundamental compromises. Because all drugs are poisonous at some level, the least possible amount should be administered. On the other hand, drugs are diluted in the blood stream, and large amounts are degraded, excreted, or adsorbed onto healthy cells; so the doses must be large enough to overcome this wastage. In some cases a compromise between these contradictory requirements is almost impossible—if a drug is administered in sufficient quantity to effect a cure, a side effect of the drug may kill the patient. However, drugs encapsulated in vesicles have been found to circulate in the blood for considerable periods without being degraded or adsorbed. Such liposomal drugs have provided effective therapy for several prevalent diseases—invariably with far smaller doses than usual. Most vesicles containing a drug

are recognized as foreign and eventually ingested by cells of the immune system that circulate in the blood stream. For this reason drugs encapsulated in vesicles-one may think of them as medical Trojan Horses-have proven effective in treating infections of the immune system itself. The vesicles may also be incorporated into body tissue in other ways; for example, the lipid bilayer composing the vesicle may become fused with a cell membrane. Such fusion allows liposomal drugs to be adsorbed by cells that are not part of the immune system and to provide effective therapies for diseases such as fungal infections. Finally, weakened pathogens concentrated on the surfaces of vesicles can induce the immune system to produce antibodies, making liposomal vaccines promising candidates for disease prevention.

We don't always understand why liposomal drugs work, and probably no single hypothesis will explain all successes. Nevertheless, an increased understanding may well come from a knowledge of the morphological changes that occur both when vesicles are diluted in the blood stream and when they come into contact with living matter. Clearly if the "wrong" phase change takes place when a liposomal drug is diluted in the blood-for example if the vesicles transform into open sheets and release their drug prematurely-encapsulation will have been in vain. For this reason neutron-scattering studies of vesicle structures are an important element in the development of liposomal drug-delivery systems.

Here at the Los Alamos Neutron Scattering Center. Rex Hjelm has made extensive studies of spontaneous vesicle formation in a mixture of the bile salt g]ycocholate and lecithin suspended in water. Such spontaneous liposome formation could greatly reduce the costs of drug-delivery systems. The morphologies of particles formed in the
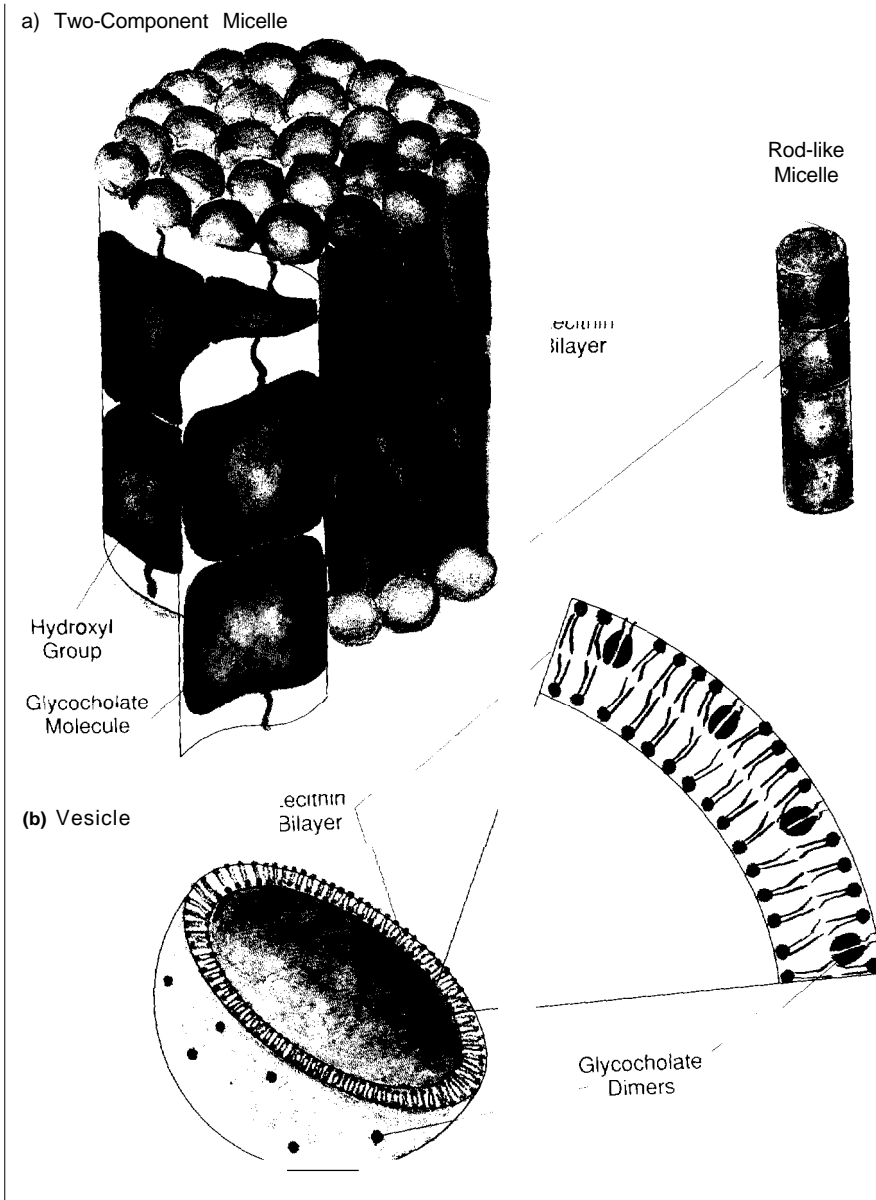
PARTICLES INVOLVED IN FAT DIGESTION

Fig. 4. Depending on their concentration in aqueous solution, molecules of the lipid lecithin and the bile salt glycocholate form a variety of structures. (a) At high concentrations and high molar ratios of glycocholate to lecithin, globular particles form. The lecithin molecules form bilayers with their hydrophobic tails (red) pointed inwards and their hydrophilic heads (blue) exposed to the aqueous environment. It is thought that the glycocholate molecules stabilize the bilayers by forming a "ribbon" two molecules wide that wraps around the particle, further isolating the lecithin tails from the water. The hydrophilic, hydroxyl-containing surfaces of the glycocholate molecules form the outside of the ribbon. Neutron-scattering data show that the particles are 50 angstroms high and 50 angstroms in diameter and suggest that they assemble into long rods as the system is diluted. Particles of this kind are thought to occur naturally in the liver and the gall bladder for the purpose of removing lipophilic products—cholesterol, for example-from the liver. (b) When the concentration of glycocholate drops below a critical level as a result of dilution, vesicles form. Less glycocholate is available to associate with the lecithin, and the two-component micelles in (a) are no longer stable. Instead it is thought that the glycocholate molecules form dimers that act as wedges within the lecithin bilayer, causing it to curve and form a hollow sphere, or vesicle, The precise details of this dramatic rearrangement are not yet known. Such vesicles are thought to occur naturally in the digestive tract, emulsifying dietary fats and thus enhancing the effects of digestive enzymes.

glycocholate-lecithin system depend on a number of factors, including concentration; thus a knowledge of how the particles evolve from micelles at high concentrations to vesicles at low concentrations is essential to the development of liposomal drugs. The glycocholate-lecithin system is all the more interesting as it is an essential component in the digestion of fat from mammalian diets. Although glycocholate and lecithin are both amphiphilic, the glycocholate is far more soluble, and the combination of the two seems more efficient for solubilizing fats in the digestive tract than either alone. The emulsification of fats by the glycocholate-lecithin combination appears also to enhance the action of digestive enzymes.

A peculiarity of the glycocholate-lecithin combination is that the particles it forms tend to grow larger as the system is diluted in water, down to a low concentration at which they transform to vesicles. Such behavior is opposite to the usual effect of dilution. As Hjelm and his collaborators added water to their glycocholate-lecithin system they observed that the form of the neutron scattering law had changed in a manner qualitatively consistent with a change from globular micelles to rod-like structures. However, attempts to fit the data to the scattering law of a population of uniform-sized cylindrical micelles were not very successful; evidently, cylinders of different sizes were present in the suspension. To find out the size distributions of the particles, Hjelm and Devinderjit Sivia used a method of analysis known as the maximum entropy method. They assumed the system contained cylindrical micelles whose radii and heights could take any value within a reasonable range and calculated the neutron scattering law for each combination of radius and height. Then they applied the maximum entropy method to the observed

scattering law to determine the best estimate of the number of micelles with each height and radius. (Their results are plotted as equi-population contours in Fig. 11 of "Bayesian Inductive Inference, Maximum Entropy, and Neutron Scattering.") At a concentration of 16.7 grams per liter, most of the particles had globular structures with heights centered at 50 angstroms and radii centered at 25 angstroms. At a concentration of 10 grams per liter, a new population of elongated particles emerged in addition to the first group. Remarkably, the second population had about the same mean radius as the first but twice the mean height. Finally, on dilution to 7.1 grams per liter, a third population with a height three times greater than the first began to emerge. Since a lecithin bilayer is about 50 angstroms thick, these data strongly indicate that the elongated particles are built up of disks composed of lecithin bilayers. At present, Hjelm and his collaborators believe the glycocholate molecules wrap like a ribbon around the circumference of the lecithin disks (Fig. 4).

Polymer Colloids. Association colloids such as micelles and vesicles are not the only type of colloids in our arsenal of modem materials. In another type of colloid called a *latex,* the core of each particle consists of long polymer molecules. Latices were first produced by a process called emulsion polymerization as part of the development of synthetic rubber during World War 11. In emulsion polymerization, droplets of monomers of an insoluble synthetic resin are kept in colloidal suspension by the addition of a suitable surface-active agent, or *surfactant,* composed of amphiphilic molecules. To this emulsion is added a small quantity of free-radical polymerization initiator, which diffuses through the surfactant shell and causes the monomers within to polymerize. The process produces a colloidal disper-

sion of polymeric, synthetic-resin microsphere, each surrounded by a surfactant layer that prevents their aggregation. At moderate particle concentrations, this dispersion has the appearance of a milky, white liquid.

Latex particles of different sizes and size distributions can be produced for a variety of industrial applications. For example, the particles may be dried to form a continuous film of latex paint, paper coating, carpet backing, or adhesive. They may also be used as pigments, as length calibration standards for electron microscopy, and as carriers for antigens in diagnostic immunological tests. To improve the latices—to design a better paint, for example—it is essential to have a detailed understanding of the process of emulsion polymerization and an accurate characterization of the structural and chemical properties of the latices that are produced, Without such knowledge design of new materials is a hit-and-miss affair.

Different characteristics of latices are important for different technologies, and no single investigative technique can provide a complete description of all particle properties. However, many of the properties of importance are structural. Examples include the mean particle size, the morphology of particles with more than one component ("avocado" or "current bun," for example), the type of force between particles, the thickness of the amphiphilic stabilizing layer that surrounds each particle, and the texture of the particle surface (rough or smooth). Once again, much of this information can be obtained by small-angle neutron scattering. Over the last decade, university and industrial researchers have performed a number of small-angle neutron-scattering experiments to determine the distribution of particle sizes in dilute latices containing one type of polymer. This information may be obtained either by fitting the scattered-neutron intensity to an as-

sumed distribution of particle diameters or by using the maximum entropy method to determine the most probable distribution. In either case, neutron scattering provides a simple alternative to the laborious counting of latex particles in electron micrographs. Results from these two techniques usually agree well. Contrast matching has also been used successfully to determine both the composition and structure of copolymer particles, that is, of particles formed from two different types of polymer molecules. Such information cannot be obtained by any other means.

To determine the composition of the particles of a copolymer latex, researchers collect SANS data for suspensions of the latex in various mixtures of H_2O and D_2O. Because $I(0)$, determined by extrapolation from the Guinier plot described earlier, is proportional o $(\bar{\rho}_p - \bar{\rho}_s)^2$—the square of the difference between the average scattering-length density of the particles and the average scattering-length density of the solvent—a graph of $\sqrt{I(0)}$ versus $\bar{\rho}_s$ yields a straight line (Fig. 5). The intersection of that line with the $\bar{\rho}_s$ axis (the point at which $I(0) = 0$, or the contrast-matching point) is equal to $\bar{\rho}_p$. For example, the data in Fig. 5 lead to a value for $\bar{\rho}_p$ of 4.94×10^{10} cm^{-2}. The composition of a copolymer latex may then be obtained directly by solving the following equation for c:

$$\bar{\rho}_p = c\rho_A + (1 - c)\rho_B, \qquad (3)$$

where c is the fraction of polymer A in each particle and $(1 - c)$ is the fraction of polymer B. The quantities ρ_A and ρ_B are the scattering-length densities of polymer A and polymer B, respectively. They can be deduced from the scattering lengths of the atoms in the molecules and their known molecular volumes. Alternatively, experimental values for ρ_A and ρ_B can be obtained by measuring the contrast-matching points
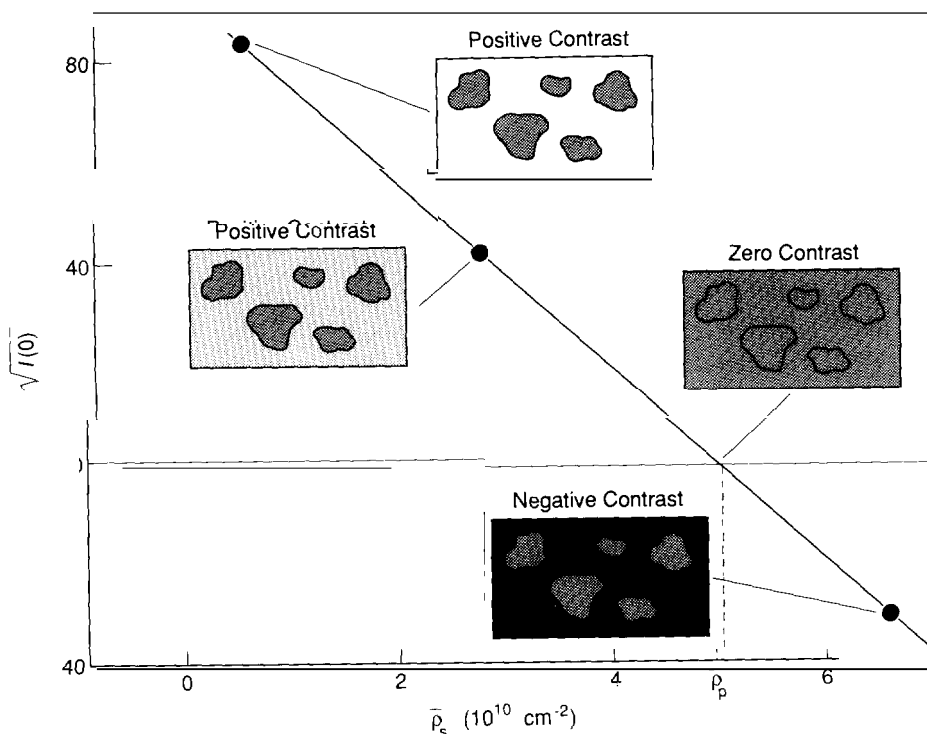
DETERMINING THE COMPOSITION OF A COPOLYMER LATEX

Fig. 5. Neutron-scattering data for copolymer-latex particles dispersed in water can reveal the relative amounts of the two polymers (here polystyrene and polyacrylonitrile) in the particles. The intensity of the neutrons scattered through zero degrees, $I(0)$, is proportional to the square of the scattering contrast, $(\bar{\rho}_p - \bar{\rho}_s)^2$, where $\bar{\rho}_p$ is the average particle scattering-length density and $\bar{\rho}_s$ is the average solvent scattering-length density. Thus, a graph of $\sqrt{I(0)}$ versus ρ_s should be a straight line, and the intersection of that line with the ρ_s axis (the point at which $\sqrt{I(0)} = 0$ and hence $\bar{\rho}_p = \bar{\rho}_s$) equals $\bar{\rho}_p$ for the latex particles. The three data points shown were obtained by varying the percentage of D_2O in the water; for two of the data points the contrast is positive $(\bar{\rho}_p - \bar{\rho}_s > 0)$, and for the third the contrast is negative $(\rho_p - \rho_s < 0)$. We can then use Eq. 3 in the text to determine the relative amounts of polystyrene and polyacrylonitrile in each particle. The data shown correspond to latex particles containing 63.6 percent polystyrene and 36.4 percent polyacrylonitrile. (Data courtesy of R. H. Ottewill of the University of Bristol.)

of latices prepared from the individual polymers.

In many cases it is possible to adsorb molecules—such as paint pigments or drugs-onto the surfaces of latex particles. To determine how many molecules are adsorbed under different chemical conditions, SANS measurements are first performed on bare particles in a series of solvents of different contrasts

in order to determine the scattering-length densities of the particles. Then the molecules of interest are adsorbed onto the latex particles, and the scattering law for the composite particles is measured in a solvent whose scattering-length density equals that of the latex particles alone. The observed scattering law is due to the shell of adsorbed molecules only. By fitting the observed

scattering law to that expected for a spherical shell. the total amount of adsorbed chemical may be determined. If the molecules are absorbed into the latex rather than *adsorbed* on the surface. the particles usually swell. Absorption can be discriminated from adsorption because a contrast-matching point can be found for uniform swollen particles but not for particles with a core-and-shell morphology.

Polymers

Of course, polymer molecules do not occur only as constituents of latex particles dispersed in a solvent. Most often in our everyday experience, an assembly of polymers is a solid lump-a telephone housing or a fishing pole-rather than a constituent of a milky liquid. Depending on the chemical composition of' the polymer molecules and the method of preparation, a bewildering variety of mechanical, electrical. and optical properties can be achieved. in many cases the properties depend sensitive) on the organization of the polymer molecules. that is. on the local molecular structure (Fig. 6). For example, a fiber made of Kevlar is very difficult to break because the polymer molecules in the fiber are stretched out along its length rather than being coiled around like tracks in a labyrinth. The strength of the Kevlar fiber is determined to a significant extent by the strength of carbon-carbon chemical bonds along individual polymer molecules. Fibers made of coiled polymer molecules, on the other band. tend to stretch and break when pulled because the polymer molecules are only weakly linked and tend to slide over one another.

We know that individual polymer molecules are made of' several thousand repeated subunits, called monomers. and that they are very long; an average polymer with a molecular weight of' 200,()()() daltons has a stretched length of several

(a) UHMWPE Gel

(b) UHMW PE Fibers

ULTRA-HIGH-STRENGTH FIBERS
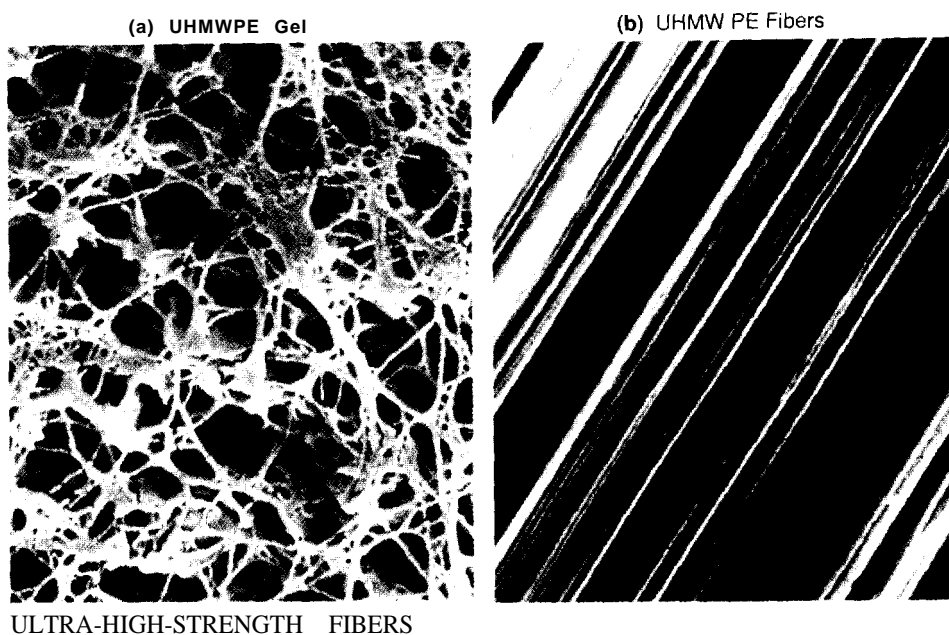
Fig. 6. The tensile strength and stiffness of fibers made from ultra-high-molecular-weight polyethylene (UHMW PE) depend on the extension and alignment of individual polymer molecules—properties that depend, in turn, on the degree of polymer cross-linkage in the gels from which the fibers are formed. (a) A 2-percent solution of UHMW PE molecules was cooled to form the gel shown in this scanning electron micrograph (magnification = 1000). The structure of the gel reflects agitation of the solution prior to cooling. (b) This scanning electron micrograph shows a dried gel from a 0.6-percent solution of UHMW PE that has been drawn to 130 times its original length. (The draw direction was diagonal.) Note the extremely high degree of orientation. Over the last decade advances in techniques for manipulating the structures of UHMW PE gels by changing conditions and concentrations of the original solutions have led to rapid increases in the tensile strength of commercial fibers. (Micrographs courtesy of Paul Smith, University of California, Santa Barbara.)

microns (1 micron = 10,000 angstroms). But the long molecules are not usually stretched out unless special techniques have been used for synthesis, so how are they usually arranged'? Before neutron scattering answered this question in the early seventies, there were several competing theories. One was based on a random coiling of the polymer molecules-much like a plate of well-mixed spaghetti. Another held that a large traction of the polymer molecules were quasi parallel over some large fraction of their length.

According to the random-coil model, the radius of gyration of a polymer

molecule-which is a measure of the length of the molecule just its the diameter of' a loosely wound ball of' wool is a measure of the length of wool in the ball-ought to be proportional to the square root of the molecular weight of the polymer if the polymer is suspended in an *ideal solvent,* one that supports molecules rather than changing their conformation. Neutron-scattering researchers tested this prediction using small-angle scattering. Once again, the technique of selective deuteration allowed them to see a few select polymer molecules winding through a conglomeration of many others-essentially

the deuterated polymer molecules stood out from the background of their hydrogenated brethren just as a strand of spinach spaghetti would stand out in a plate full of the normal variety. The radii of gyration obtained by neutron-scattering experiments of this type for many different polymers were in impressive agreement with the prediction of the random-coil model. However the argument did not conclusively prove the model correct because it could not rule out a significant degree of local molecular alignment. To investigate this point, neutron-scattering data had to be obtained at greater values of Q, between about 0.1 and 0.6 inverse angstroms, where the conformation of the molecules is probed over distances smaller than their size, that is, between 10 angstroms and 50 angstroms. The idea was to see if polymer molecules line up with each other along segments within that size range. Comparisons of such data and calculations based on the random-coil model showed very good agreement for a variety of amorphous polymers and no indication of quasiparallel packing.

Fractal Objects

Many of the objects encountered in sludge science are disordered—polymers and ceramics, for example. Such materials seldom display the translational and rotational symmetries encountered in crystals and so cannot be characterized geometrically by such concepts. Fortunately a type of geometry called fractal geometry can be applied to the description of many disordered materials. Moreover, neutron scattering can be used to study objects that exhibit this type of geometry.

Fractal geometry was introduced almost two decades ago by Benoit Mandelbrot to describe objects—such as trees, clouds, mountains, and lakes—that cannot be described by normal Eu-

clidean geometry because their surfaces or coastlines are too "bumpy." Mandelbrot's central observation was that many of the objects whose structure he sought to describe are self-similar when dilated (Fig, 7). For example, if we magnify a piece of coastline on a map, the image we obtain looks very much like the original. Small inlets now look much like fjords, and fjords have become ocean. Similarly, under dilation small islands in an archipelago look like the larger ones on the original map, but the overall appearances of the enlarged and original maps are very similar. This type of self-similarity is usually referred to as *statistical* to distinguish it from the exact dilational symmetry displayed by geometrical patterns such as the Sierpinski gasket. Statistically self-similar objects-clouds for example—look approximately the same under dilation.

Self-similarity is an appealing concept, and one can easily list examples of self-similar, or fractal, objects from many fields of study: blood vessels, lungs, tree bark, lightning, and galaxies are obvious candidates. But how do we say something exact about them? The answer was provided many years ago by Hausdorff and other pure mathematicians who had no idea that their theorems would be applied to natural phenomena. They examined how some measure of an abstract object, such as the distance between elements of the object, changes with the length scale on which this property is examined. This basic idea is easily applied to concrete examples such as the coastline of Norway. Suppose we try to measure the length of this jagged coastline. Clearly, if we use a long "ruler" we will jump across fjord entrances and get the wrong answer. To avoid this problem we could use a shorter ruler. But since the coastline is self-similar we will still jump over some inlets—they will just be smaller than the ones we missed with the larger ruler. Of course

we could continue this process *ad nauseam,* using smaller and smaller rulers, but because the coastline is self-similar, the total length we measure will always depend on the length of the ruler we use. Such a result clearly has no place in Euclidean geometry! However, if we use enough different rulers, we eventually find that the length of the coastline is proportional to the ruler length raised to the power $(1 - D)$, where D is called the *fractal dimension* of the coastline. For the coastline of a Euclidean object, such as a triangle, the fractal dimension is unity—the usual Euclidean dimensionality of a line—so its length is (fortunately for Euclid) independent of the length of the ruler used to measure it. The fractal dimension of the Norwegian coastline is about 1.2, illustrating that D is not usually an integer for fractal objects.

The concept of fractal dimension can also be applied to "solid" objects. The mass m of a sphere of uniform density scales as the cube of its radius r: $m = \frac{4}{3}\pi\rho r^3$. What about the mass of a spherical hunk of foam or a porous rock? Such a self-similar structure contains a great deal of "air"; so its mass fractal dimension—the power of a single dimension that is proportional to the object's mass—will be less than three. By the same token, a fractally rough surface has a larger area than a smooth surface; so its fractal dimension is greater than 2, the Euclidean dimension of smooth surfaces.

Materials scientists use fractal geometry because many growth and aggregation processes tend to form disordered systems that can only be characterized as fractal. Even simple polymers are fractal: according to the random-coil model of polymers mentioned earlier in this article, the mass of a polymer in an ideal solvent scales as the square of its radius of gyration; its mass fractal dimension is 2. Other examples range from dendrites in metals to glasses. Of-

(a) Sierpinski Gasket

(b) Fractal Coastline

× 2'   × 2²   × 2⁵

x 2*   × 2¹²   × 2¹⁶

× 2²⁰   × 2²⁴   x l
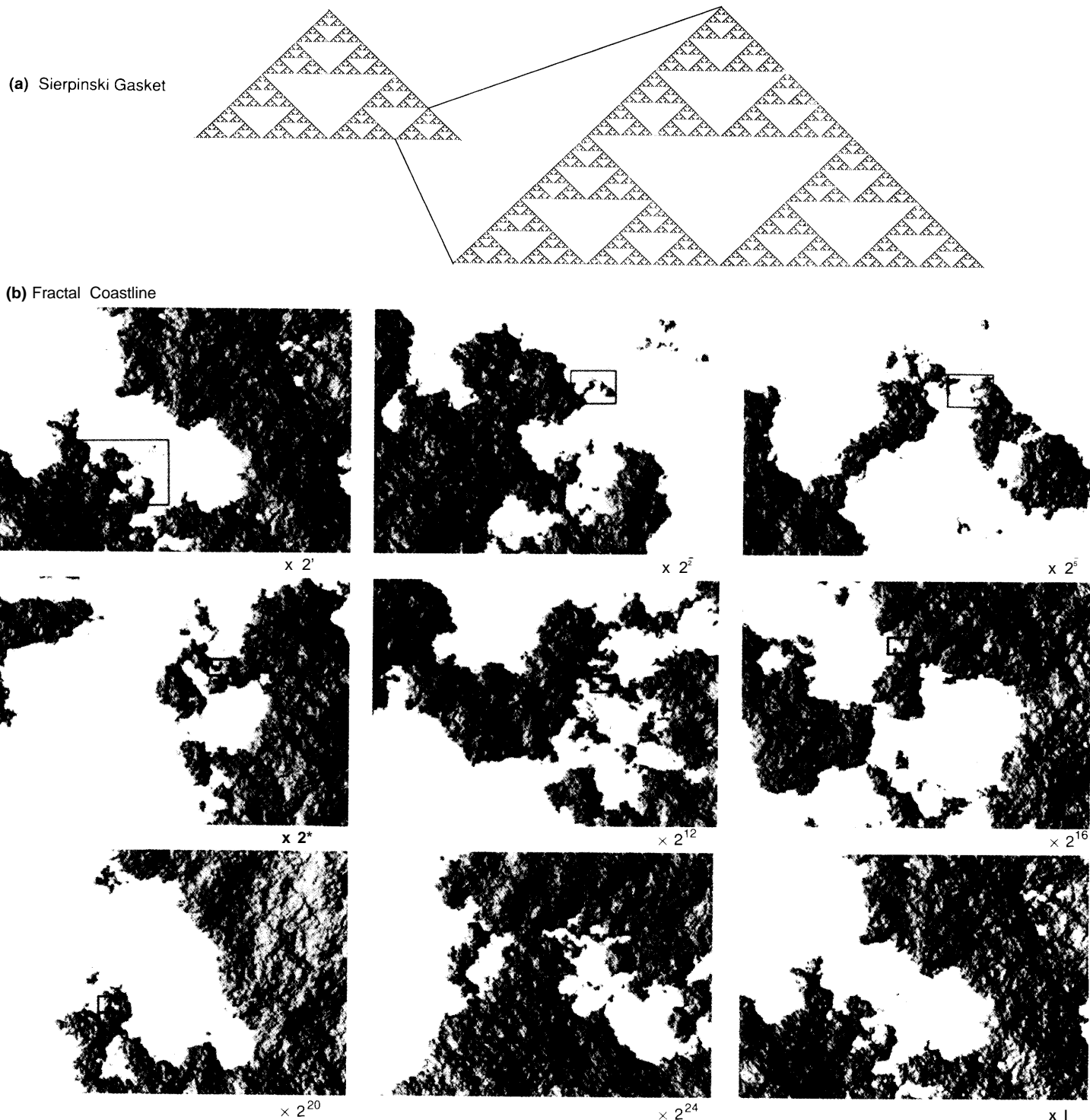
SELF-SIMILARITY

Fig. 7. The concept of self-similarity is essential to fractal geometry. (a) In the exactly self-similar pattern known as the Sierpinski gasket, any upright, triangular section of the pattern can be be made identical with any other upright, triangular section by dilation or shrinking. (The pattern is assumed to repeat indefinitely.) Obviously the maps shown in (b) do not display such exact dilational symmetry—it is impossible to expand one and overlay it exactly on another. On the other hand, enlargement of the part of each figure inside the small box gives the suceeding figure, and one can easily imagine that both figures are part of the same map. (The original map appears at the end of the series of enlargements to show that this similarity exists between coastlines of any magnification.) Such shapes are called statistically self-similar. The algorithm used to generate these pictures, called fractal Brownian motion, is similar to that employed by film-makers who wish to draw realistic mountains and lakes. (Fig. 8b @Richard Voss/IBM Research.)

ten fractal patterns appear in systems that develop far from thermal equilibrium. For example, under non-equilibrium conditions aggregating particles may stick to a growing cluster at positions other than those that would yield the lowest free energy, whereas at thermal equilibrium particles tend to bounce around until they find those positions. For this reason open, dispersed structures are formed rather than the compact crystalline structures typical of growth under equilibrium conditions (Fig. 8). The type of structure produced depends to a large extent on the details of the non-equilibrium growth process. Materials researchers have begun simulating such growth processes on computers (Fig. 9) and comparing the structures the simulations produce with the structures of samples produced in carefully controlled experiments. The essential grounds for comparison are the fractal dimensions of the structures. Neutron and x-ray scattering are ideal techniques for measuring the fractal dimension of macromolecular structures because they can probe length scales ranging from interatomic distances to the sizes of many molecular aggregates (Fig. 10). Furthermore the scattering laws for fractal systems are simply power laws— the scattered-neutron intensity is proportional to Q raised to some power. For mass fractals the exponent is equal to $-D_m$, where D_m is the mass fractal dimension of the scattering object, whereas for compact objects with fractally rough surfaces, the exponent is equal to $6 - D_s$, where D_s is the fractal dimension of the surface. Thus, for fractal objects encountered in sludge science, the slope of a plot of the logarithm of scattered-neutron intensity versus the logarithm of Q is simply related to D_m and D_s. By comparing experimental values of D_m with those predicted by different growth models, the growth process in each experiment can be inferred. Because no naturally
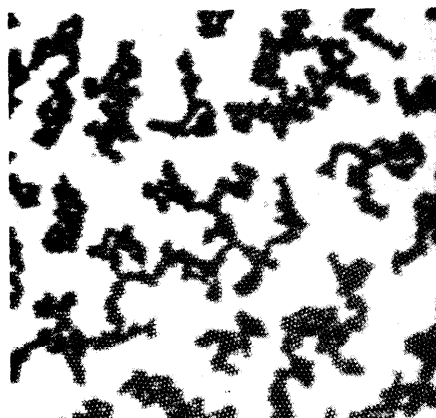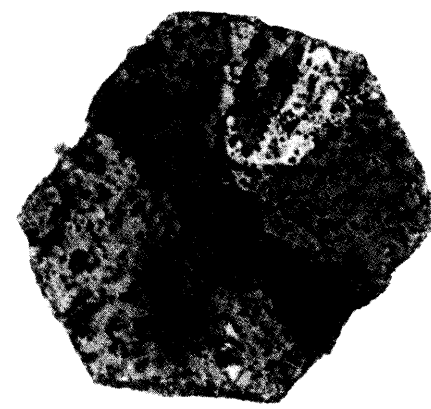

$$\frac{d\bar{r}}{dt} = 2 \times 10^{-2} \ \mu m/s$$
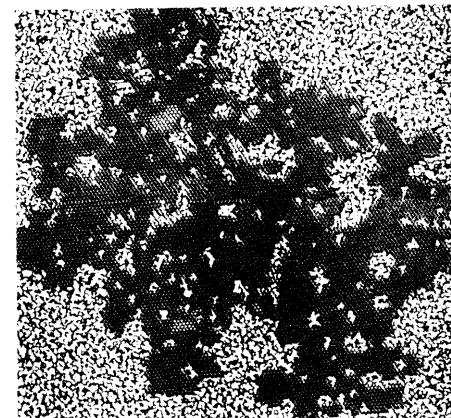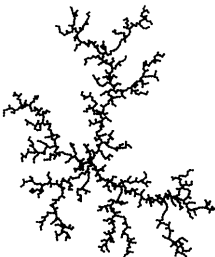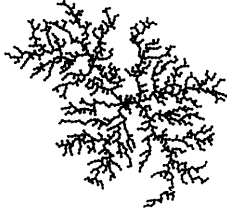
$$\frac{d\bar{r}}{dt} = 3 \times 10^{-4} \ \mu m/s$$
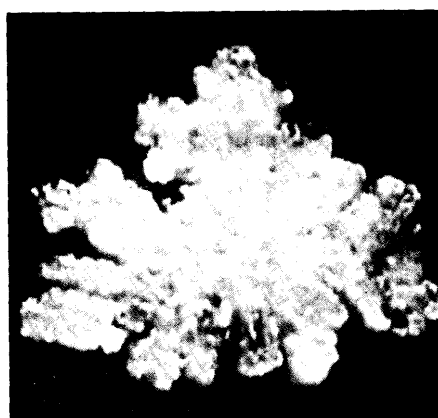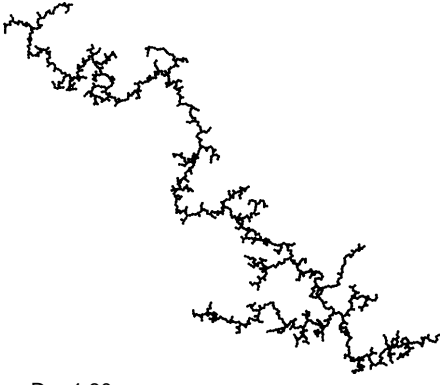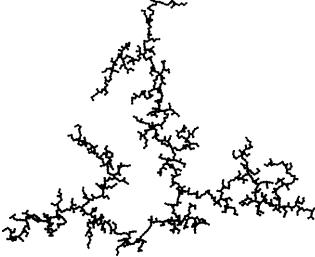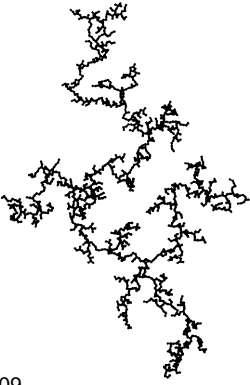
$$\frac{\partial r}{\partial t} \approx 1 \times 10^{-5} \ \mu m/s$$

$$\frac{d\bar{r}}{dt} \approx 5 \times 10^{-6} \ \mu m/s$$

PRODUCTS OF DIFFERENT AGGREGATION RATES

Fig. 8. In an elegant experiment with simple equipment, Skjeltorp was able to show that the form of aggregated matter depends sensitively on the speed of accretion. A colloid of negatively charged, 1.1-micron-diameter plastic spheres was suspended in water and placed on a microscope slide, together with a few 5.5-micron spheres. When a cover slip was placed over the drop, the larger spheres acted as spacers, defining a single layer within which the smaller spheres moved in a Brownian fashion as a result of collisions with water molecules. By adjusting the salinity of the colloid, Skjeltorp was able to control the repulsion between the spheres, and thus the rate of accretion. With a small repulsive interaction, particles tend to stick together when they collide; with a larger repulsive interaction, the particles undergo many collisions, exploring configurations of different total energy before finding one that lowers the energy of the system enough to allow accretion. Thus, larger repulsive interactions correspond to slow growth under conditions close to thermal equilibrium. The figure shows micrographs of the aggregates produced and the rate of change of average radius for each aggregate. (The crystalline aggregate took over six months to form.) Experiments like this one provide a visual framework for interpreting the fractal dimensions of molecular aggregates, data which can be obtained by neutron-scattering experiments. This experiment was reported by Arne Skjeltorp in "Visualization and characterization of colloidal growth from ramified to fractal structures" (Physical*Review Letters* 57, p. 1444 (1987)).

Diffusion-Limited Aggregation	Ballistic Aggregation	Reaction-Limited Aggregation

Monomer-Cluster Growth

Witten and Sander	Void	Eden
D = 2.50	Ɔ = 3.00	D = 3.00

Cluster-Cluster Growth

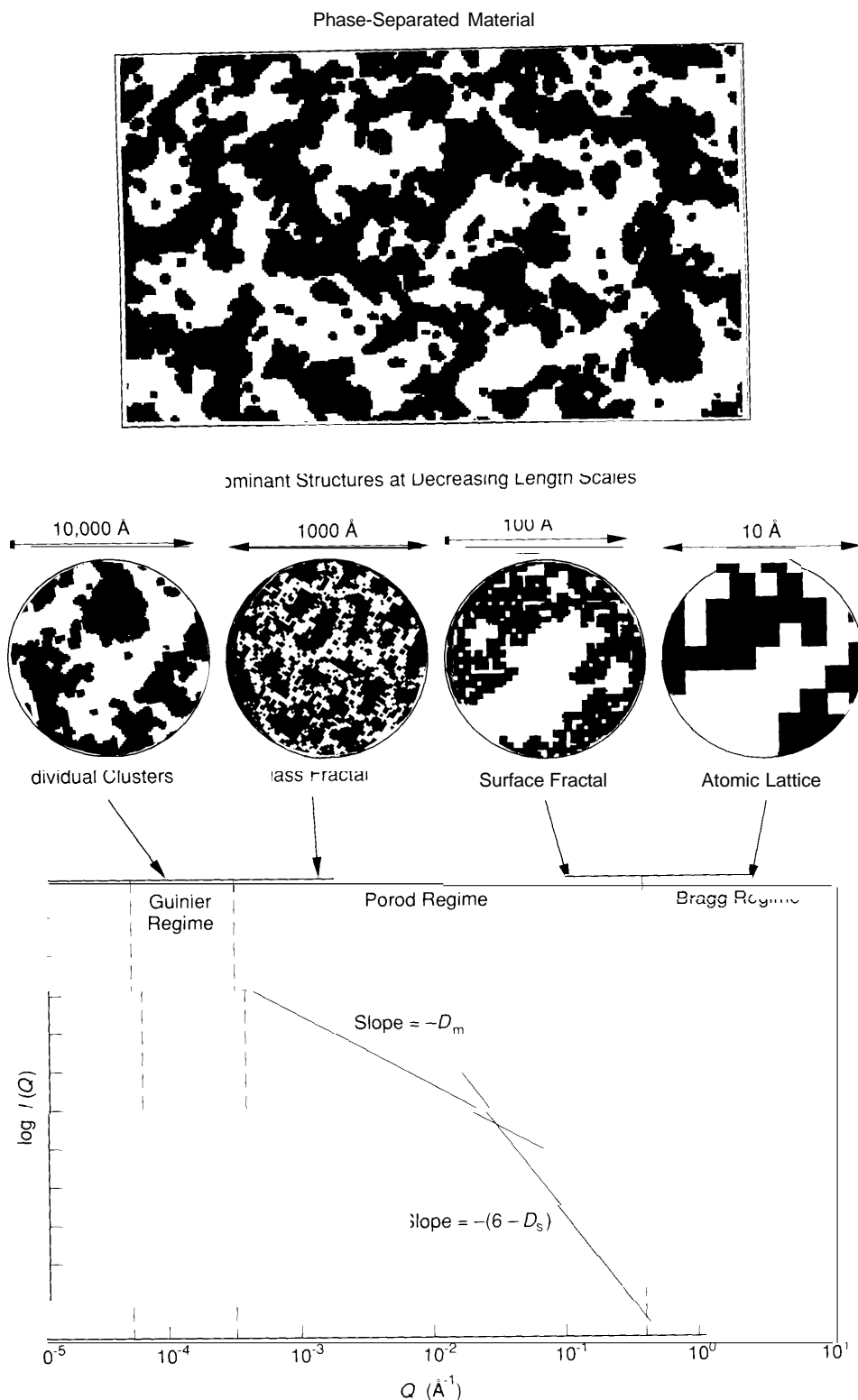| DLCA	Sutherland	RLCA
D = 1.80	D = 1.95	D = 2.09

COMPUTER MODELS OF NON-EQUILIBRIUM GROWTH PROCESSES

Fig. 9. Computer simulated non-equilibrium growth processes produce three-dimensional structures with characteristic mass fractal dimensions (their two-dimensional analogs are shown here). Diffusion-limited aggregation (DLA), invented by Witten and Sander, simulates growth by placing a seed particle, or monomer, at a point on a grid and allowing other, similar particles to diffuse inwards from the edges of the grid in a series of random steps. The cluster, initially represented by the seed, grows if a particle lands on a site next to it. Because the particles move randomly, few of them ever penetrate to the interior of a growing cluster and accretion takes place at the tips. This so-called monomer-cluster growth results in a highly ramified structure with a mass fractal dimension of 2.5. An even more open structure, with a fractal dimension of 1.8, is formed by cluster-cluster growth, that is, if the growing DLA clusters are allowed to move around and aggregate with each other. The ballistic growth model invented by Void—which is applicable to some gas-phase growth processes—assumes the same aggregation conditions as DLA, except that the particles travel in straight-line, or ballistic, paths before sticking to a cluster. Thus some penetrate to the center of the growing cluster, and a more compact aggregate is formed. Again, if clusters are allowed to move and aggregate, a more open structure is formed. Reaction-limited aggregation, which was invented by Eden, simulates growth in which some chemical barrier to aggregation, rather than the type of particle motion, determines when a particle sticks to a cluster. Thus a particle must land on sites next to the growing aggregate several times before sticking, and extremely compact particles are formed. Again, if clusters are allowed to move and aggregate, a more open structure is formed. Most branched polymers in solution follow reaction-limited kinetics. The important point to note is that the fractal dimensions of the clusters, and the visual impressions they give, vary considerably with the growth conditions. (Figure courtesy of Paul Meaken; reprinted with permission from Kluwer Academic Publishers.)

occurring object can be self-similar under dilation of arbitrary magnitude, a straight-line plot is obtained only over a range of Q values corresponding to the specific length scale of self-similarity. For example, the aggregates shown in Fig. 9 can be self-similar only on length scales between the size of an individual particle and the size of a cluster.

Fumed Silica. Alan Hurd and his collaborators have successfully used neutron- and light-scattering techniques combined with computer growth models to investigate the growth of fumed silica particles. This material is prepared commercially by burning $SiCl_4$ in hydrogen and oxygen to produce highly ramified silica clusters, which are used to modify

the flow properties of foods and paints. (Next time you visit your local supermarket check the ingredients of common foods. It is not unusual to find that one of the ingredients is silica—sand by another name!) A similar process is used to make the starting materials for optic fibers. By conducting scattering experiments on samples obtained from
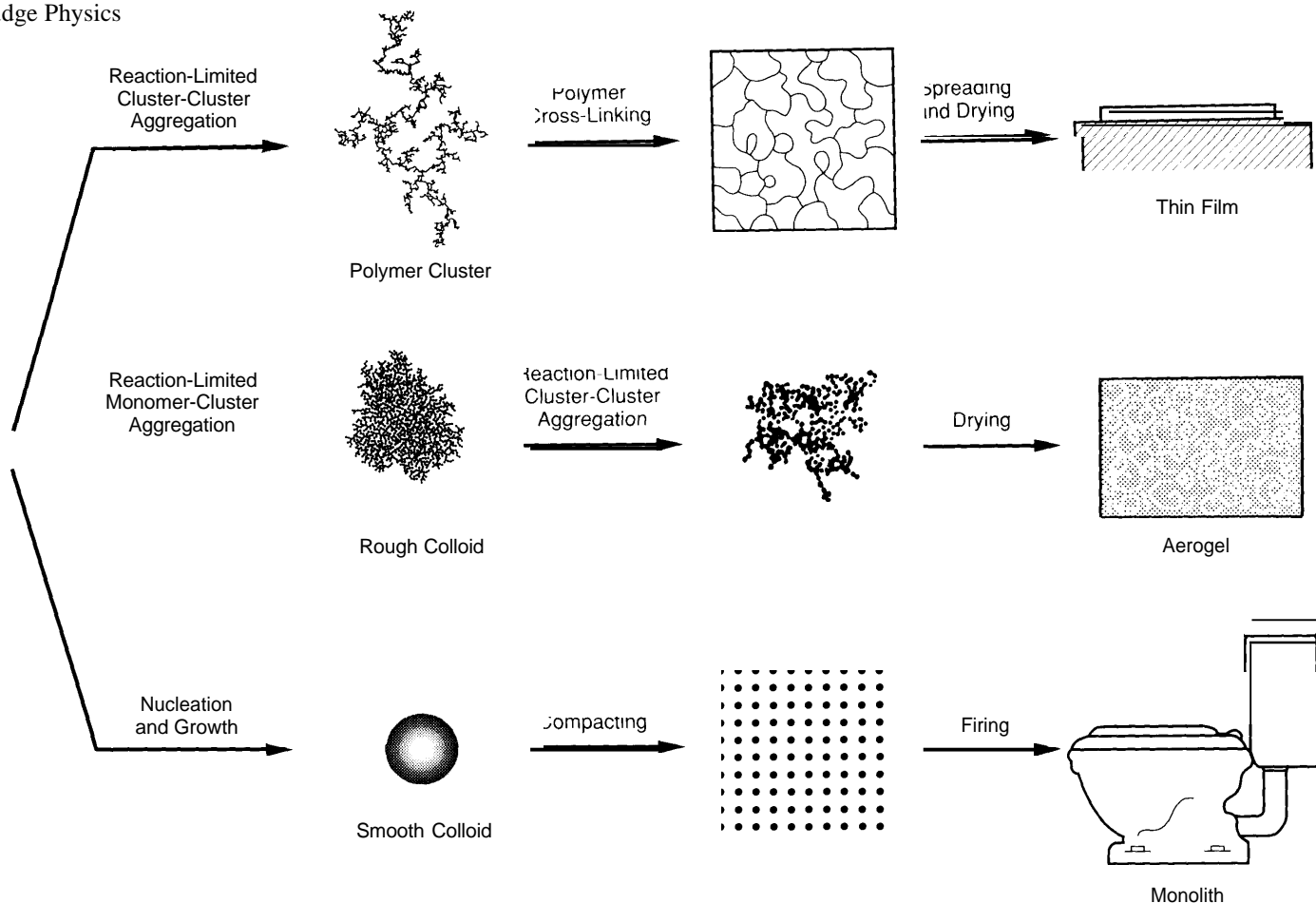
Phase-Separated Material

ominant Structures at Decreasing Length Scales

| 10,000 Å | 1000 Å | 100 Å | 10 Å |

dividual Clusters | ass Fractal | Surface Fractal | Atomic Lattice

SCATTERING LAWS AT DIFFERENT LENGTH SCALES

Fig. 10. The black and white regions represent single-phase fractal clusters that are assumed to have separated from a highly disordered material by a non-equilibrium process. The shape of the scattering law for the phase-separated material (plotted as $\log I(Q)$ versus $\log Q$) changes as Q increases because the material's nonuniformity is being probed at different length scales. Small values of Q probe long length scales, whereas large values of Q probe short length scales. In the inner region, where $QR \sim 1$, the scattering law measures the overall cluster size R of each phase. As Q increases, the internal fractal structure of the clusters is probed, and a scattering law of the form Q', where D_m is the mass fractal dimension, is observed. When Q exceeds a value close to the inverse size of the holes in the fractal clusters, the surfaces of the aggregates are probed, and the scattering law changes to the form $Q^{(6-D_s)}$, where D_s is the surface fractal dimension of the clusters. Finally, at large values of Q, the scattering pattern evolves to a form containing Bragg peaks, which are characteristic of structural variations on atomic length scales. (Adapted from a figure in an article by Dale Schaefer. *Proceedings of the Royal Society of London* A423:37, 1989.)

SiC1$_4$/H$_2$/0$_2$ flames, Hurd and his collaborators deduced that three processes are involved in the formation of fumed silica particles. In the early stages of growth SiO$_2$ monomers aggregate to form compact, rough-surfaced clusters resembling those produced by the ballistic monomer-cluster aggregation process (Fig. 9) and grow to sizes approaching 100 angstroms. Because the flame temperatures are near the melting point of silica, annealing competes with aggregation and the particles become smoother as they grow. Later in the growth process, when no more monomers are present, these smooth particles tend to coalesce, forming micron-sized aggregates whose fractal dimensions characterize

Reaction-Limited
Cluster-Cluster
Aggregation

Polymer Cluster

Polymer
Cross-Linking

Spreading
and Drying

Thin Film

Reaction-Limited
Monomer-Cluster
Aggregation

Rough Colloid

Reaction-Limited
Cluster-Cluster
Aggregation

Drying

Aerogel

Nucleation
and Growth

Smooth Colloid

Compacting

Firing

Monolith

CERAMIC PRODUCTS AND THEIR PRECURSORS

Fig. 11. Depending on the initial conditions of growth, precursor particles made from a single monomer can lead to final products with widely varying properties. Reaction-limited cluster-cluster aggregation under acidic catalysis conditions yields polymerized precursors with a fractal dimension of 2.09. The highly ramified polymers then cross-link to form gels that collapse on drying into hard, high-density films. Such films are used as insulating layers in integrated circuits, and research is under way to use them as ferroelectric, nonvolatile computer memory-elements. Reaction-limited monomer-cluster aggregation forms compact, rough-surfaced colloidal particles, which then aggregate through cluster-cluster growth. Because the gels so formed are denser and much stronger at short length scales than those already discussed, they do not collapse when dried but rather form extremely porous, diaphanous materials called aerogels. Researchers hope to exploit the high surface area of aerogels to make transparent materials for insulating passive solar walls; however, present production costs are too high. In the traditional method of producing hard, durable, ceramic material for everyday use, smooth colloidal particles are grown under near equilibrium conditions, compacted, and then fired. (Adapted from a figure in *Science* 243 (1989): 102.)

them as products of the diffusion-limited cluster-cluster aggregation process.

The importance of experiments like those carried out on fumed silica is that they provide an understanding of the relationship between growth conditions and the structures of the aggregates produced (Fig. 11). Materials scientists can use this information to tailor growth conditions and produce the structures required for particular applications. For example, silica aggregates, similar in chemical composition to the fumed silica described in the previous paragraph, can be produced in solution by polymerization of silicic acid. Depending on the pH of the reaction bath, how-

ever, quite different structures are produced. Catalysis of the reaction under acidic conditions produces a highly ramified, polymeric silica with a mass fractal dimension of about 2 by the reaction-limited cluster-cluster aggregation process. This silica collapses easily on drying and produces high quality protective films. On the other hand, a rough-surfaced, compact, colloidal silica, which is formed under basic catalysis conditions by the reaction-limited monomer-cluster process, is resistant to collapse and much more suitable for the production of porous, high-surface-area materials. Once again we see that an understanding of structure, which can

be provided by neutron scattering, is a prerequisite for the development of strategies for material preparation.

Composite Materials. Composites are multi-component materials in which an attempt is made to retain the useful properties of each component. For example, fumed silica is often combined with silicone elastomers to increase the strength of the elastomer while retaining its elastic properties. Figure 12 shows some typical experimental results obtained by Dale Schaefer and his collaborators at Sandia National Laboratories. The lower curve shows that the elastic modulus of pure polydimethyl-
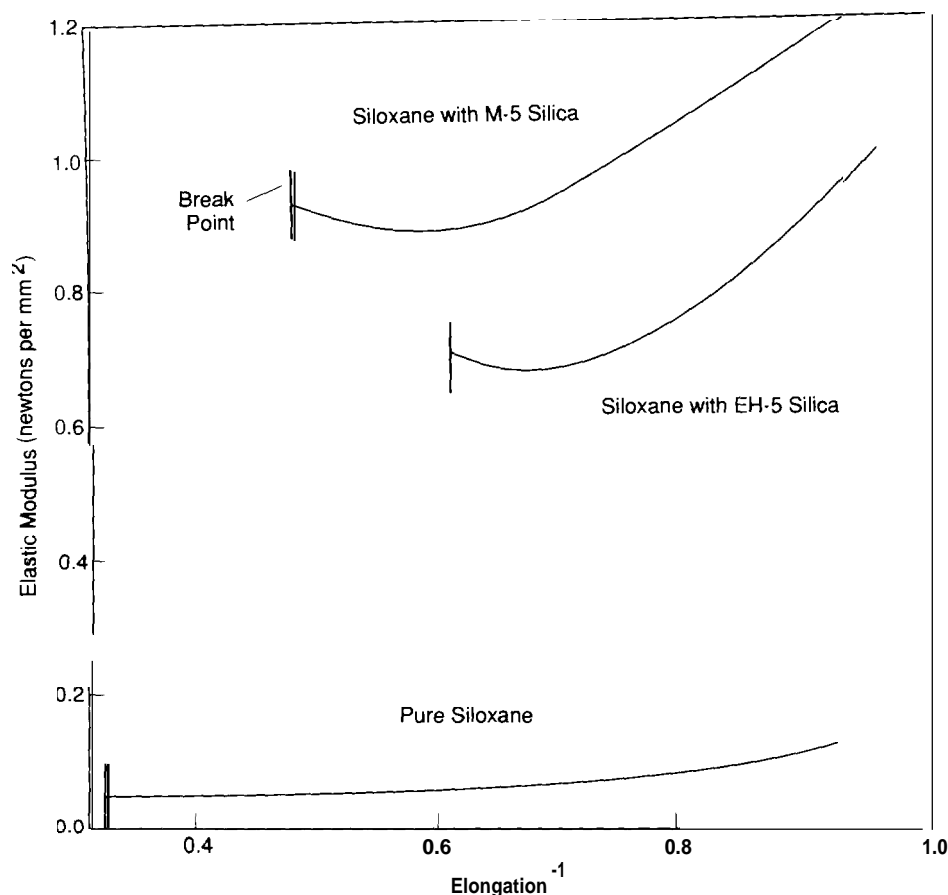
STRENGTH OF SILICA-SILOXANE COMPOSITES

Fig. 12. The properties of siloxane composites containing fumed silica as a reinforcing agent vary widely depending on the structure of the fumed silica particles. Pure siloxane rubber can be stretched to approximately four times its original length before it breaks. It also has a low elastic modulus, so little force is required to stretch it. (Elastic modulus is defined as the ratio of the applied force per unit cross-sectional area to the elongation, where the elongation equals the ratio of the change in length to the original length.) Pure siloxane rubber also grows progressively weaker as it stretches. Siloxane reinforced with rough-surfaced EH-5 fumed silica has a higher elastic modulus and breaks at a much lower elongation than pure siloxane. Smooth-surfaced M-5 fumed silica is a better reinforcing agent; it forms a composite that has a somewhat higher elastic modulus and breaks at an intermediate elongation. Researchers had expected composites of siloxane and the rough-surfaced EH-5 to perform best. They now think that particle size may be a more important property than surface texture because M-5 particles are larger than EH-5 particles. In addition, the higher-temperature growth process that smooths the surfaces of the M-5 particles may also strengthen them and hence the composite rubber. (Figure courtesy of Dale Schaefer, Sandia National Laboratories.)

siloxane is small and becomes smaller as the material is elongated (that is, as we move left along the horizontal axis). A small elastic modulus means the material stretches with little applied force. After three-fold elongation the material breaks—there are no further data points to the left. When the elastomer is reinforced with two types of fumed silica, M-5 and EH-5, much higher elastic moduli are found, but the composite materials break at smaller elongations than does the pure "rubber." Scattering data show that the M-5 fumed silica has a smooth surface whereas the EH-5 fumed silica has a rough surface. Therefore, the elastic modulus data indicate that smooth silica particles produce better reinforcement than rough ones—a somewhat counterintuitive result. Similar studies are underway at LANSCE to examine the relationship between the structures of carbon blacks—usually thought of as amor-

phous forms of carbon—and the properties of the rubber produced when carbon black is used as a reinforcing agent. Information obtained in these investigations is potentially of great economic importance-a decrease of 1 percent in the fuel consumption of automobiles due to improvement in tire rubber is worth a billion dollars or more every year!

Molecular composites differ from the conventional variety described above in that the filler is generated *in situ* during production rather than by mixing. Multiphase materials of this type, in which the phases are dispersed at the 100-angstrom level, offer great possibilities for the enhancement of material properties, but it is difficult to design materials until the relationship between synthetic protocol, structure, and properties has been established. A case in which these relationships have. been investigated is that of composites made by swelling a polydimethylsiloxane rubber with tetraethylorthosilicate and polymerizing the swelled material to produce SiO_2—that is, glass—precipitates. This process was pioneered by J. E. Mark at the University of Cinncinati. The structure of the precipitated silica turns out to be very sensitive to chemical conditions prevailing during the synthesis, and the resulting silica and rubber composites vary significantly in elasticity and strength. Under some conditions, scattering experiments show that a bicontinuous network of glass and rubber is formed by a process called spinodal decomposition, yielding brittle composites. Under different chemical conditions the glass filler appears to have a polymeric mass-fractal character that enhances the extensibility of the resulting composite. Those who have studied molecular composites of this sort admit that they are often wrong in their intuitive guesses about the relationship between filler morphology and the mechanical properties of the resulting composite. There is no substitute for a

careful cataloging of the relationships between synthetic protocol, structure, and properties.

Surfaces

Earlier in this article I described a way of using small-angle neutron scattering to examine particle-like structures formed by amphiphilic molecules. Complementary information concerning surface structures formed by amphiphilic molecules can be obtained from neutron reflectometry by adsorbing the molecules on a liquid and reelecting neutrons from the air-liquid interface (see "Neutron Scattering—A Primer" for an account of neutron reflectometry). As is so often the case, substitution of deuterium for hydrogen in both the molecules and the liquid increases the power of neutron scattering for such studies. One can even make the liquid a mixture of H_2O and D_2O that does not reflect neutrons at all, so that only the amphiphilic molecules at the surface are visible to neutrons! Both the amount of material adsorbed at the surface and many of the structural properties of the surface layer can be determined by reflectometry. For example, measurements on a variety of amphiphilic molecules show that the adsorbed layer usually consists of three principal regions. The first, nearest the vapor, contains only hydrocarbon chains; the second contains a small fraction of chains, the negatively charged head groups, solvent, and a few cations such as Na^+; the final region contains solvent and a diffuse. atmosphere of ions. The thickness of each region can be established by reflectometry, as can the fractions of the various components in each region. When the. thickness of the first region is less than the length of the hydrocarbon chains, an average tilt angle for the chains can sometimes be determined. The strong resemblance these layers bear to one side of the lipid bilayer discussed ear-

lier suggests that neutron reflectometry can be used to study model biological membranes; indeed, such studies have already started at several facilities.

Block copolymers—polymers made up of a string of monomers of one type (block A) linked to a string of monomers of another type (block B)—are used as surfactants, compatibilizing agents in polymer blends, and adhesives in biomedical and microelectronics applications. Very often the individual polymer blocks segregate, giving rise to heterogeneous arrangements consisting either of alternating layers *(lamellae)* or of rods of one block embedded in a matrix composed of another block. Such structures are often disorganized in bulk samples, making them very difficult to study. For example, the lamellae may be broken up and disorganized with respect to their neighbors. [n copolymer films, on the other hand, one or other polymer block usually has an affinity for the film surface; thus lamellae are formed in an ordered way, parallel to the surface of the film. Neutron reflectometry is an ideal tool for investigating such copolymer films because the contrast variation technique, implemented through selective deuteration, can be used to highlight one or the other of the polymer blocks.

The copolymer films studied so far at LANSCE (and other neutron-scattering centers) are formed by placing a drop of solvent containing the copolymer on the surface of a silicon wafer and spinning the wafer at high speed to produce a uniform, thin film of copolymer as the solvent dries. The film is a random alloy of its polymer components at this stage, with both polymer blocks thoroughly mixed and entangled (see Fig. 13). When the polymer film is annealed, however, the different polymers segregate into alternating layers parallel to the plane of the film. The layers tend to form first at the top and bottom surfaces of the film. and the

sequence of layers propagating from each surface depends on the affinity of each polymer for the interface in question. Thus, if the system has a lower free energy when polymer-block A attaches to the silicon substrate than when polymer-block B does, the order will be A,B,A,... away from the substrate surface. The fully annealed film produces a complicated reflectivity profile from which it is possible to deduce the layer thicknesses as well as the definition and shape of the interfaces between adjacent polymer blocks. What happens during the annealing process to resolve the competition between the order of layers propagating from each face of the film is still somewhat of a mystery and the subject of continuing investigation at LANSCE and elsewhere.

Such studies of polymer compatibility bear on the crucial economic and environmental problem of recycling plastics. In 1984 the U.S. produced 46.3 billion pounds of plastics and discarded 18 billion pounds of plastic wastes. Recycling of the wastes would not only save disposal costs but would also reduce energy consumption; it is estimated that producing a fabricated plastic from waste instead of virgin resin would result in an 80-percent saving of energy. Unfortunately, it is not easy to make different plastics compatible. Various strategies such as using block copolymers to knit together incompatible homopolymers or using "radiation grafting" to form new materials from incompatible plastics have been proposed. To find out how well those techniques work, one may use neutron reflectometry to study the molecular structure of interfaces so formed between different polymers. The same message that we have seen in other areas is once again clear, but in a slightly different form. In this case, we need to understand the relationship between structure and properties in order to invent a new way of processing plastics.
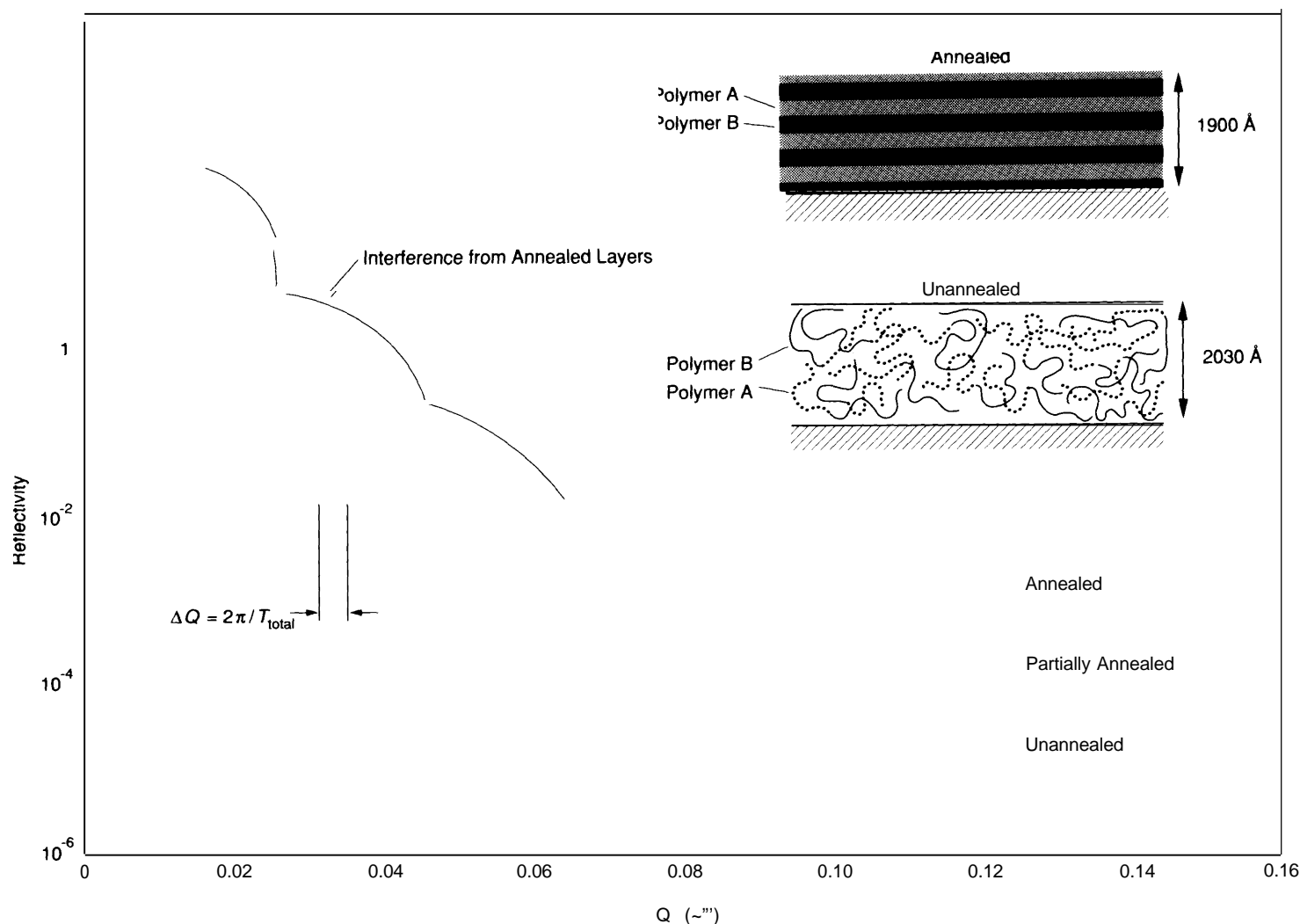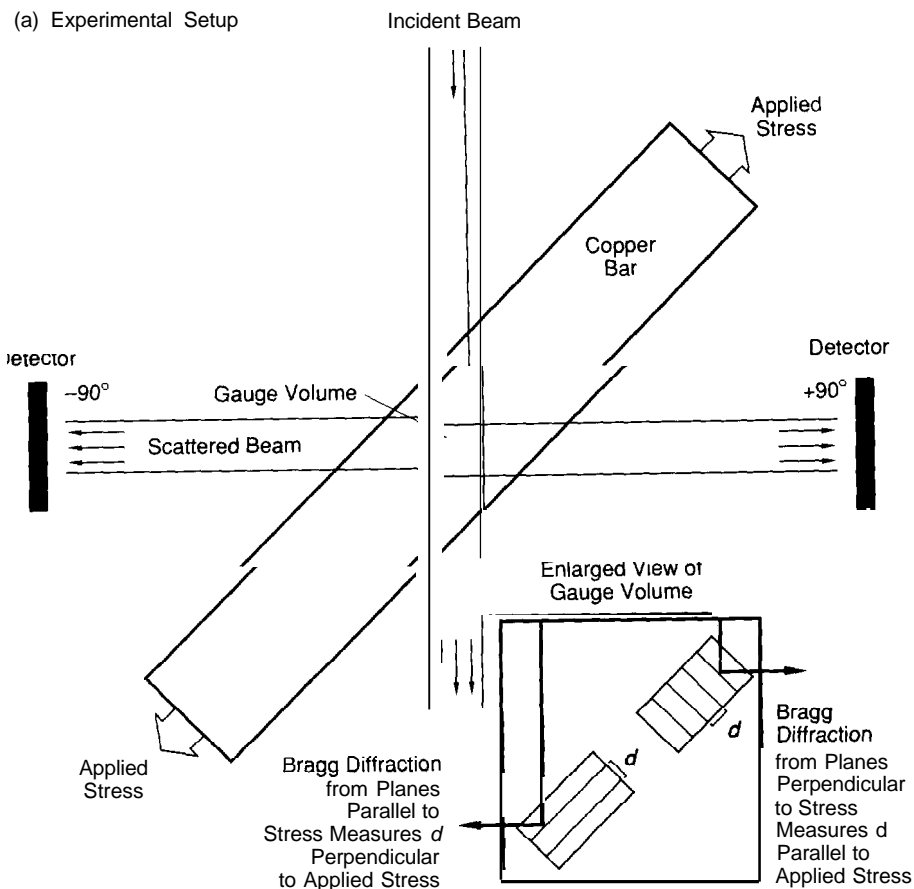
NEUTRON-REFLECTOMETRY MEASUREMENTS ON A BLOCK-COPOLYMER FILM

Fig. 13. Neutron-reflectivity profiles at three stages of the annealing of a diblock-copolymer film reveal the gradual formation of alternate layers of polymer A (polystyrene) and polymer B (polymethylmethacry late). (Two of the profiles have been shifted vertically for easier reading.) The reflectivity profile of an unannealed, homogeneous film is a series of evenly spaced peaks of decreasing amplitude (an interference fringe pattern) produced by the interference of neutron waves reflected from the film's top and bottom surfaces. The difference between the C? values at which successive peaks occur, ΔQ, is inversely proprtional to T_{total}, the thickness of the homogeneous film. The data shown here indicate a thickness of 2030 angstroms for the unannealed film. The reflectivity profile for the fully annealed film (heated for 24 hours at 170°C) indicates a series of alternating microphage layers, each made up of a single polymer. The closely-spaced ripples due to interference from the whole film are superimposed on a new series of broader interference peaks (suggested by hairlines above the curve) due to the layers formed during annealing. Secondary-ion-mass-spectroscopy measurements indicated that each of these layers contained only one polymer and had a thickness of about 250 angstroms. Neutron-reflectometry measurements helped elucidate the long-range order and the degree of interpenetration of polymer layers. The alternating layers of polymer A and polymer B form because like polymers have an affinity for each other and tend to segregate together. (The bottom and top layers are half the size of the intermediate layers because they are formed from only one polymer block.) The reflectivity profile for a partially annealed film shares features of the other two. These measurements are part of a series of experiments to elucidate the processes and spatial relationships that dictate the final order. (The measurements were taken at LANSCE for Tom Russell of IBM.)
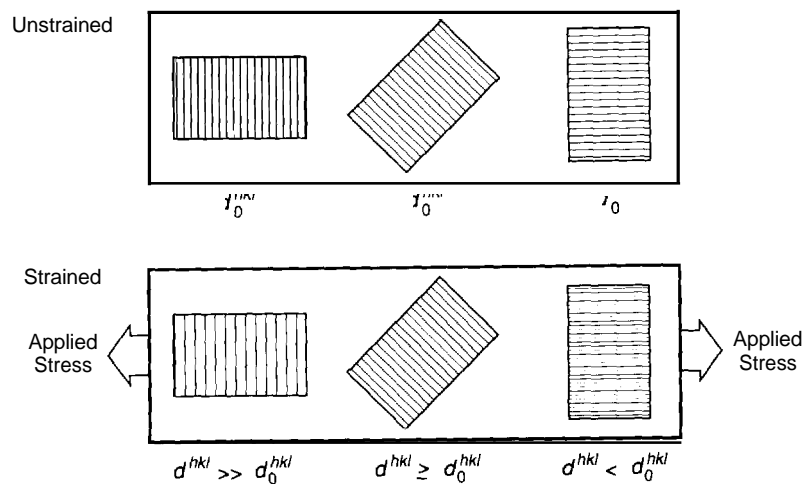
(a) Experimental Setup

(b) Expected Changes in Lattice Spacing Resulting from Applied Stress

Unstrained

Strained

$d^{hkl} \gg d_0^{hkl}$ $d^{hkl} \geq d_0^{hkl}$ $d^{hkl} < d_0^{hkl}$

Residual Stress—A New Application of Neutron Scattering

Residual stresses—or residual forces per unit area-can be introduced into mechanical components both by fabrication processes and by deformations that occur during use. Any operation involving nonuniform deformation or thermal gradients—forging, welding, bending, and machining, for example—can give rise to residual stress. Whether [he stresses are detrimental or beneficial to the strength and durability of' a component, however, depends on the direction and magnitude of' forces applied during use. In general, a residual stress that adds to an applied stress is detrimental to performance, whereas one that reduces the applied load is beneficial. For example, thick-walled pipes for a variety of applications in the chemical, nuclear, and armament industries are often subjected during use to a variety of cyclic internal pressures. Such tubes are frequently fabricated with compressive residual stresses on the inside, close to the bore, to inhibit crack propagation and extend lifetimes.

Anyone trying to predict the behavior- of a mechanical component would want to know the distribution of residual stresses; however, most of the methods available for obtaining this information involve destruction or modification of the component—rather obvious drawbacks. An alternative, nondestructive method uses x-ray or neutron diffraction to determine local values of strain-that is, changes in the spacings between planes of atoms in the crystal. Stresses are then deduced from well-known relationships between stress and strain. At a spallation neutron source such as LANSCE. the deformation is determined by measuring the difference between the wavelengths of neutrons that diffract through a given scattering angle from a given set of planes in both stressed and unstressed samples. The differ-

ent wavelengths are directly related to changes in the spacings of the atomic planes and thus to strains in various directions. Since the materials of interest are polycrystalline, Bragg peaks can be observed for any sample orientation unless the individual crystal grains exhibit considerable preferred orientation.

Depending on their application, the x-ray- and neutron-diffraction techniques each have unique advantages. X rays

are very useful for measuring surface strains; however, they do not penetrate most engineering materials sufficiently to be useful f-or bulk measurements. Neutrons, on the other hand, penetrate well in most cases—20,000 times farther than x rays in iron, for example—and so provide a nondestructive method of determining lattice distortions, or strains, throughout relatively large engineered components. Because the distor-

(a) Neutron-Diffraction Data
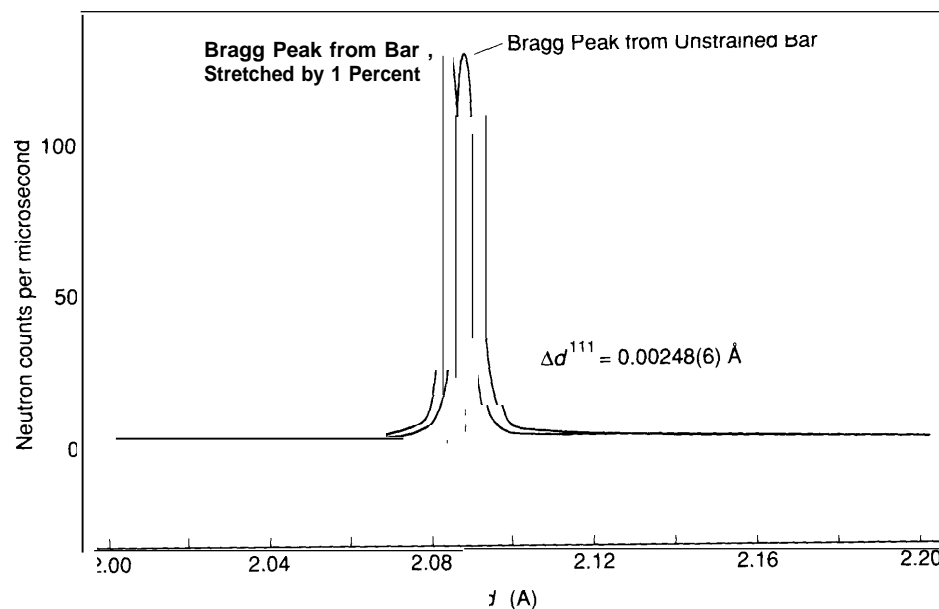
MEASURING STRAIN WITH NEUTRON DIFFRACTION

Fig. 14. Neutron diffraction can determine the strain in a polycrystalline material by measuring the stress-induced changes in the lattice spacings of crystallite, that is, in the spacings between sets of parallel planes of atoms. (a) Shown here is the experimental setup for measuring the strain in a copper bar stretched along its length. The bar is oriented at 45 degrees relative to the incident neutron beam and neutrons diffracted through ±90 degrees are detected. As shown in the blowup of the gauge volume (the volume in which lattice spacings are measured), this setup implies that the Bragg peak from a certain set of planes parallel and perpendicular to the applied stress are recorded in the -90 degrees and the +90 degrees detectors respectively. The lattice spacings d between those planes are related to the wavelength, and hence time of flight, of the neutrons that make up the Bragg peak. (b) Applied stress along the copper bar is expected to increase the lattice spacing between planes perpendicular to the applied stress and decrease the lattice spacing between planes parallel to the applied stress. Here d_0^{nkl} is the lattice spacing of the (hkl) planes in three variously oriented crystallite of an unstrained bar, and d^{hkl} is the lattice spacing of the same set of planes after the sample has been strained. The indices (hkl), called Miller indices, uniquely identify the set of lattice planes being measured.

(b) Strain-Induced Changes in Lattice Spacing

Set of Lattice Planes (hkl)	$(d - d_0)/d_0$ for Planes ⊥ to Stress	$(d - d_0)/d_0$ for Planes ∥ to Stress
111)	+0.119(3) %	−0.097(7) %
200)	+0.209(3) %	−0.150(5) %
220)	+0.130(4) %	−0.117(3) %
222)	+0.113(5) %	−0.112(13) %

## MEASUREMENT OF STRAIN IN A STRETCHED COPPER BAR

Fig. 15. To determine the microscopic elastic strains in a copper bar stretched by 1 percent, researchers compare the Bragg peaks for a certain set of planes before and after applying stress. (a) The position of the Bragg peak for the (111) planes shifts by an amount corresponding to a change in the (111) lattice spacing of 0.00248(6) angstroms. (The number in parentheses is the uncertainty in the last digit(s).) (b) The table summarizes the percentage change in lattice spacing, or $(d - d_o)/d_o$ for four sets of planes. The change is positive when the sets of planes are perpendicular to the applied stress and negative when the sets of planes are parallel to the applied stress, as expected. Note that the percentage changes in the lattice spacings of parallel sets of planes, the (111) and (222) planes, are equal within the experimental error, as they should be. Sets of planes that are not parallel to each other show different strains because copper is elastically anisotropic. The strain measurements were made on the Neutron Powder Diffractometer at LANSCE.

tions occur on the scale of interatomic distances—that is, on a much smaller scale than the 100 to 1000 angstroms covered by small-angle neutron scattering and neutron reflectometry-and because the materials of interest are polycrystalline, powder diffraction is the technique of choice.

Figure 14a shows the arrangement for measuring strains in a stressed copper bar with a neutron powder diffrac-tometer. The intersection of the incident and detected neutron beams defines the so-called gauge volume, the volume of material within which the average inter-planar spacings are measured. By using suitable neutron-absorbing masks the gauge volume can be varied. A large gauge volume yields a high neutron count rate and thus high accuracy in the measurements, but it also yields an average value of the strain over that volume, an average that will not re-flect the true strain in regions of steeply changing stress. Typically, gauge vol-umes of a few tens of cubic millimeters provide a reasonable compromise be-tween those two factors.

The intersection of the incident and detected beams also determines the di-rection in which strain is measured. For example, as shown Fig. 14a, the detec-tors at +90 degrees and −90 degrees

Measured Region

1 inch
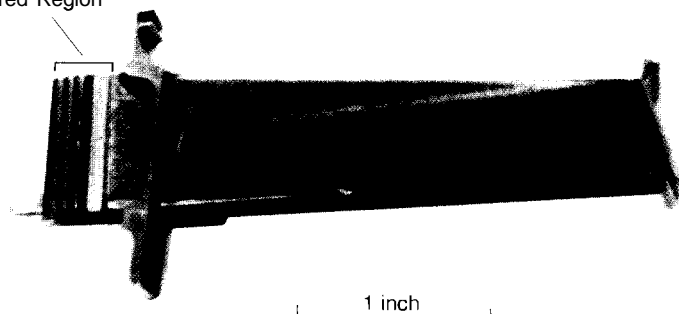
measure scattering from planes at +45 degrees and –45 degrees, If the bar is oriented as in Fig. 14, these directions correspond to lattice spacings parallel and perpendicular to the stress applied along the length of the bar. Because the copper bar is polycrystalline, there are crystallites in which a given set of lattice planes is oriented parallel to the applied stress and others in which the same set of planes is oriented perpendicular to the stress. In general, one would expect the lattice spacings to increase in a direction parallel to the applied load and to decrease in the perpendicular direction. Figure 15a shows a Bragg peak shift resulting from stretching the copper bar by 1 percent, and Fig. 15b lists the changes in lattice spacing for several sets of lattice planes. As expected, the lattice spacings parallel to the stress increase while the lattice spacings perpendicular to the stress decrease. The change in lattice spacing— 0.1 percent— is much less than the macroscopic change because the bar has been plastically deformed. Neutron scattering measures only elastic strain, which is much smaller. These experiments were performed on the LANSCE Neutron Powder Diffractometer, which can measure lattice spacings with an accuracy of 1 part in 100,000 or better,

On a powder diffractometer at a reactor source it is usual (although not mandatory) to work with fixed neutron wavelength and to record different Bragg peaks by changing the position of the detector (see "Neutron Scattering—A Primer"). However. the gauge volume changes shape slightly as the detector position is changed, and correcting for such effects is not always easy, especially in cases where strain varies rapidly with position in the specimen. At a pulsed spallation source, on the other hand, researchers work with neutrons of many different wavelengths simultaneously and record several Bragg peaks in a sin-
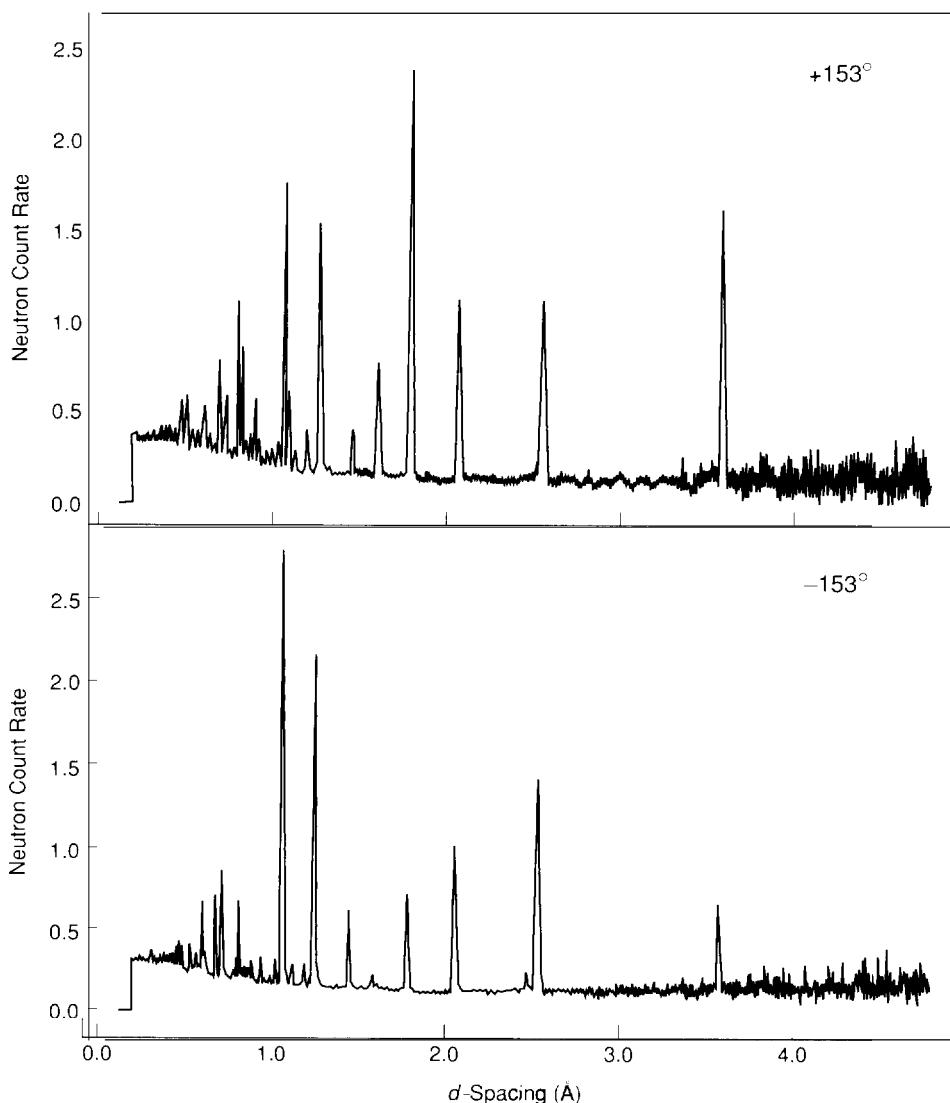
PREFERRED CRYSTALLITE ORIENTATION IN A TURBINE BLADE

Fig. 16. Bragg peaks measured at +153 degrees and –153 degrees from the incident beam of the High-Intensity Powder Diffractometer at LANSCE indicate a high degree of preferred crystallite orientation in the mounting end of a jet-engine turbine blade. If the crystalline grains were oriented randomly in the blade, the intensities of the corresponding peaks in the two patterns would be identical because equal numbers of grains would contribute to each pattern. Neutron scattering provides a simple method of checking preferred crystallite orientation.

gle detector. Because the scattering angle is constant during a measurement, the shape and size of the gauge volume are also constant. Furthermore, the simultaneous measurement of several Bragg peaks from parallel sets of atomic planes—for example, the (1 11) and (222) planes in Fig. 14—must correspond to the same microscopic strain if the measurement has been performed accurately. (The data in Fig. 14 clearly satisfy this consistency check.) Once this check has been made it is easier to be confident that the strains measured for nonparallel planes—for example, the (1 11) and (200) planes—are actually different, and that this difference is due to elastic anisotropy of the sample rather than an experimental mistake.

The Neutron Powder Diffractometer at LANSCE uses several detectors positioned symmetrically about the incident beam direction, thus allowing researchers to measure strain in several directions simultaneously. Also, by measuring a Bragg peak from the same set of planes but at several different scattering angles, researchers can determine whether the sample is textured, that is, whether the individual crystallite that make up the specimen have a preferred orientation. The data in Fig. 16 reflects the preferred orientation of the crystalline grains in a jet-engine turbine blade. The same Bragg peaks measured on the High-Intensity Neutron Powder Diffractometer at +153 and – 153 degrees ought to have identical intensities if the crystallite in the sample are randomly oriented. Instead results for the turbine blade show different intensities for each of the Bragg peaks. This occurs because turbine blades are deliberately fabricated so that all crystalline grains have the same orientation with respect to the length of blade. This direction is chosen to enhance the blade's strength and resistance to permanent deformation at high temperatures. From the variation of the intensity of

the Bragg peaks with scattering angle, one can determine the degree of crystallite orientation.

Until fairly recently experiments to determine residual stress by neutron scattering have been demonstrations only. For example, researchers have measured the stress distributions in thick-walled steel tubes, compared their results with those produced by more conventional methods of measurement, and found good agreement. In the past year or two, however, the technique has been "used in anger" for a number of measurements, including residual stress resulting from the deformation of welds, residual stress in railway lines, and residual-stress fields at the tips of propagating cracks. Future plans for work at LANSCE include measurement of residual stress in ceramics and composites, studies of stresses close to shot-peened and bearing surfaces, investigations of metals formed by compressing powders, and measurements of strain distributions around welds that have been vibrated during the welding process. The application of neutron diffraction to the determination of residual stress is a technique in its infancy and one that holds great promise for the future. ∎

Acknowledgments

Further Reading

Sow-Hsin Chen and Tsang-Lang Lin. 1987. Colloidal solutions. In *Methods Of Experimental Physics,* volume *23,* part B, edited by Kurt Skold and David L. Price, pp. 489–543. Orlando, Florida: Academic Press Inc.

Marc J. Ostro. Liposomes. *Scientific American,* January 1987, 102–111.

R. Hjelm, T. Hiyagarajan, D. S. Sivia, P. Lindner, H. Alkan, and D. Schwahn. 1990. Small-angle neutron scattering from aqueous mixed colloids of lecithin and bile salt. Accepted for publication in *Progress in Colloid and Polymer Science.*

R. H. Ottewill. 1987. Characterization of polymer colloids. In *Future Directions in Polymer Colloids,* edited by M. S. E1-Aasser and R. M. Fitch, pp. 253–275. NATO ASI Series E, volume 138. New York: Plenum Press.

G. D. Wignall. Neutron scattering. 1986. In *Encyclopedia of Polymer Science and Technology,* 2nd Edition, volume 10, pp. 112–184, Jaqueline 1. Kroschwitz, executive editor. New York: John Wiley and Sons.

Benoit B. Mandelbrot. 1977. *The Fractal Geometry of Nature. New* York: W. H. Freeman and Company.

Richard F. Voss. 1985. Random fractals: Characterization and measurement. In *Scaling Phenomena in Disordered Systems,* edited by Roger Pynn and Arne Skjeltorp, pp. 1-11. NATO ASI Series B, volume 138. New York: Plenum Press.

Dale W. Schaefer. 1989. Polymers, fractals, and ceramic materials. *Science* 243: 1023-1027.

D. W. Schaefer, B. C. Bunker, and J. P. Wilcoxon. 1989. Fractals and phase separation. *Proceedings of the Royal Society of London* A423: 35–53.

Roger Pynn and Tormod Riste, editors. 1987. *Time Dependent Effects in Disordered Materials.* NATO ASI Series B, volume 167. New York: Plenum Press.

Paul Smith. 1989. Some industrial applications of soft condensed matter in high-performance polymer processing, In *Phase Transitions in Soft Condensed Matter,* edited by Tormod Riste and David Sherrington. NATO ASI Series B, volume 211. New York: Plenum Press.

A. Stacey, H. J. MacGillivary, G. A. Webster, P. J. Webster, and K. R. A. Ziebeck. 1985. Measurement of residual stresses by neutron diffraction. *Journal of Strain Analysis* 20: 93–100.

G. A. Webster. 1989. Propagation of fatigue cracks through residual stress fields. In *Fatigue and Stress,* edited by H. P. Lieurade. Gournay-sur-Marne, France: IITT International.

D. J. Smith, R. H. Leggatt, G. A. Webster, H. J. MacGillivary, P. J. Webster, and G. Mills. 1988. Neutron diffraction measurements of residual stress and plastic deformation in an aluminum alloy. *Journal of Strain Analysis* 23: 201–211.

Samuel A. Safran and Noel A. Clark, editors. 1987. *Physics of Complex and Supermolecular Fluids. New* York: Wiley-Interscience.